3 Analysis of Transmission Loss TL(f,r) experiments conducted on the Sakhalin shelf

The first part of this section discusses the key factors influencing the variation of TL with frequency and range TL(f,r) along a shallow waveguide with uneven bathymetry. This includes the waveguide parameters as well as the influence of sea surface waves on TL. The later sections show the experimental analysis of sound propagation and TL along the proposed SEIC pipeline routes as well as the Odoptu and Chayvo areas.

3.1 Discussion of the factors controlling TL(f,r) in shallow water

The main characteristics of sound propagation on the NE Sakhalin shelf were discussed in a previous report [Kruglov et.al., 2004]. This showed that the main factors controlling sound propagation in a waveguide were the bathymetric and acoustic properties of the waveguide. Tidal internal waves were shown to cause up to 16 dB variation in the acoustic intensity of 320 Hz signals propagating along profiles oriented approximately parallel the shore. Sea surface waves were also shown to have a significant impact on sound propagation when the acoustic wavelength (λ) is less than the sea surface wave height (h)[20].

Acoustic propagation and TL data from the oil and gas production facilities to the western gray whale feeding areas are important when estimating the change in the anthropogenic noise levels in the feeding areas due to construction and development activities. Figure 3.1 is a map showing the original and alternate Offshore pipeline routes from the PA-B to the Molikpaq (PA-A) platform and onwards to the shore. A series of experimental TL profiles were acquired to investigate acoustic propagation and loss from the pipeline routes to the edge of the Piltun feeding area (PTL- profiles). Eleven profiles were acquired with lengths of more than 10 km and water depths between 20-50 m.

Industrial sources most effectively generate acoustic wavelengths shorter than ~60 m. For these wavelengths the profiled waveguides are shallow and irregular and the main factors contributing to the TL are the bathymetric profile and sea surface waves. Spatial variations in the acoustic velocity field due to the seasonal thermocline do not have a significant impact on propagation since only a fraction of the acoustic energy is carried by the high modes that are resistant to the influence of the sea surface.

[20] For example, at a frequency of 3 kHz λ =50 cm, therefore surface waves with height of greater than 0.5 m can effectively dissipate its acoustic energy and increase the TL at that frequency.

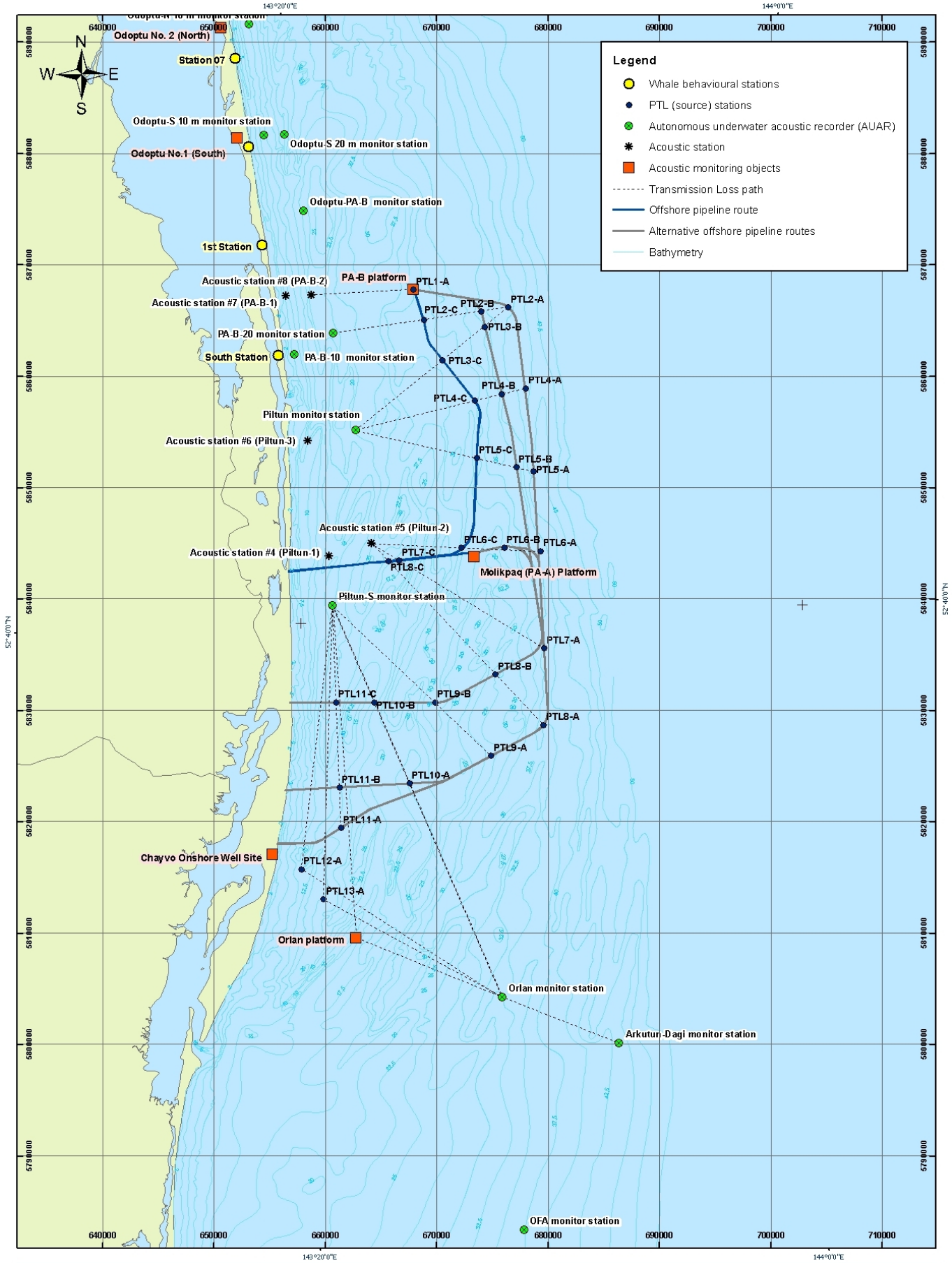

Figure 3.1 - Map of the study area showing the major facilities and pipeline routes as well as the AUAR deployment locations for the PTL experiments and the profiles surveyed.

Reflections from an irregular bathymetric profile lead to an even distribution of acoustic energy in the water layer. The spatial distribution of the sound velocity field C(z,r) and variations caused by tidal currents and internal waves affect acoustic measurements as the velocity field affects the spatial-interference structure of the acoustic field in the waveguide. The frequency and range dependent transmission loss TL(f,r) can be estimated from experimental measurements where calibrated signals are transmitted and recorded using AUARs [Borisov et.al., 2005]. The results of these experiments can be refined with modeling. Thus for a TL profile the frequency and range dependent variation in acoustic level with velocity C(z,r) can be estimated for an anthropogenic noise source.

3.2 Analysis of propagation and TL from the pipeline routes to the Piltun feeding area

Figure 3.1 is a map of the study area showing the profiles along which the TL experiments were conducted. The relationship between the names and numbers for the monitoring and acoustic stations is given in Table 1.1. The main objective of the analysis was to experimentally estimate the TL for profiles between the proposed and alternate Offshore pipeline routes and the seaward boundary of the Piltun feeding area[21]. In order to estimate the TL along a profile, AUARs are deployed at the specified monitoring stations for each profile. Tonal and broadband acoustic signals are then transmitted from the source locations for each profile. At the beginning and on completion of the transmission, hydrologic measurements were taken with the sonde. The profile was then sailed by the *Academik Oparin* with bathymetric and hydrologic measurements being taken along the profile from the TL source locations to the recording station locations.

One of the key objectives of the experimental PTL[22] measurements is to calibrate theoretical acoustic models; the acoustic and hydrologic measurements were therefore acquired in short profiles (e.g. PTL-2A is part of PTL-2) to ensure the hydrology did not vary significantly during the experiment. A bathymetric profile, a vertical hydrologic profile at the receiver location, and at each source location (both before and after transmission) as well as at intermediate points if required were acquired for each TL profile. This hydrologic sampling allowed the velocity distribution C(z,r) to be obtained along each TL profile.

[21] Piltun-S, Piltun and PA-B-20 Monitor stations, A5 and A8 Acoustic stations.
[22] Pipeline Transmission Loss profiles (numbered PTL-#) are point profiles from the proposed pipeline routes to the feeding areas. Transmission Loss Profiles (numbered TLP-#) are designed to better characterize the TL from a proposed facility and have multiple source points allowing a range dependent function to be estimated.

Figure 3.2 illustrates that the TL of acoustic energy at frequencies above 2 kHz is greatly affected by sea surface waves. Figure 3.2(a) shows the bathymetric profile and velocity distribution along TL profile PTL-11 (Figure 3.1) constructed from hydrologic measurements acquired on 4 September 2004. Figures 3.2(b) and 3.2(c) display the results of frequency dependent transmission loss TL(f) measurements conducted in calm weather (4 September) and stormy weather (26 September). Acoustic signals were transmitted from a transducer deployed at 8 m depth from the *Academik Oparin* while it was anchored at source locations PTL11-B and PTL11-A. Figure 3.2 demonstrates that the increased sea surface wave height[23] had no impact on acoustic energy at frequencies between 20-30 Hz, but significantly increased the TL at frequencies above 2 kHz. Figures 3.2(b) and 3.2(c) show that the TL(f) along the profile from PTL11-A to the Piltun-S monitor station (#5) increases with frequency at a rate approximately proportional to -19 dB/kHz at frequencies above 3 kHz, due to dissipation on sea surface waves during a storm. Figure 3.2(c) (PTL11-A and PTL11-B) shows that this effect is also proportional to profile length.

Figures 3.3 to 3.13 show the results of the analysis of the PTL experiments. Each Figure consists of two plots; one shows the bathymetry[24] and velocity C(z,r) along the profile as well as the source, receiver and intermediate hydrology locations (marked as Z1 on the plots). The second give the TL results for all the source locations for a PTL profile plotted (in different colors) on one frequency dependent TL plot.

3.3 Analysis of TL from the Chayvo Pipeline to the Piltun and Offshore Feeding Areas

In addition to the PTL experiments for the Molikpaq-PA-B pipeline routes, an experimental analysis of TL from the Orlan platform and pipeline route to the Chayvo OPF was conducted (Figure 3.1). TL studies were undertaken from the Orlan platform and two locations along the pipeline route (PTL-12, PTL-13) to the southern boundary of the Piltun feeding area and the western edge of the Offshore feeding area (Piltun-S and Orlan monitor stations).

[23] Wave height (SV) increased from <0.5 m to >1.5 m.
[24] From the sonar on the *Akademik Oparin*.

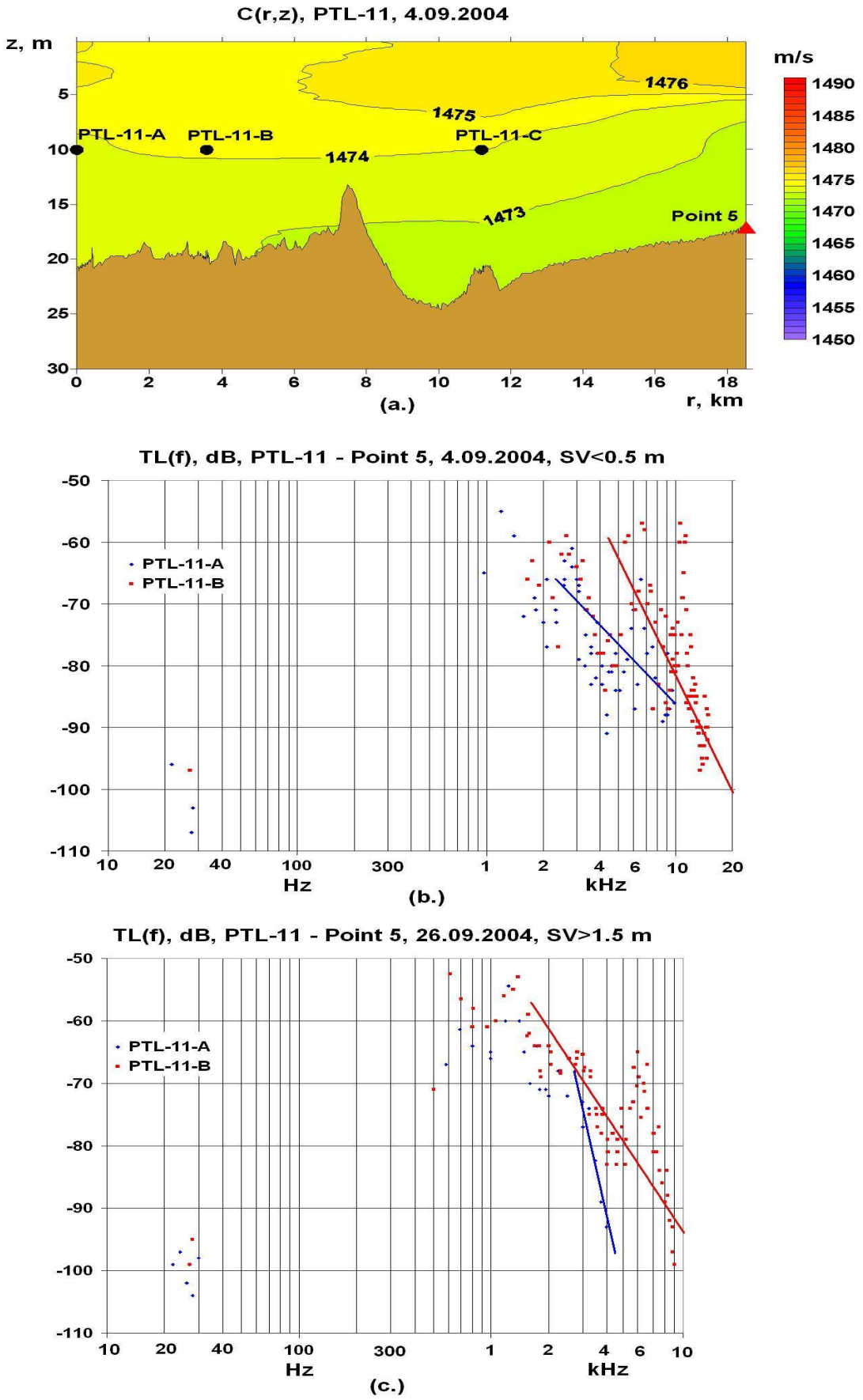

Figure 3.2 - (a) Velocity C(z,r) distribution along TL profile PTL11 and results of frequency dependent TL(f) experiments acquired in (b) Good weather and (c) Stormy weather.
(Lines represent regression of the data in the frequency range defined by the line)

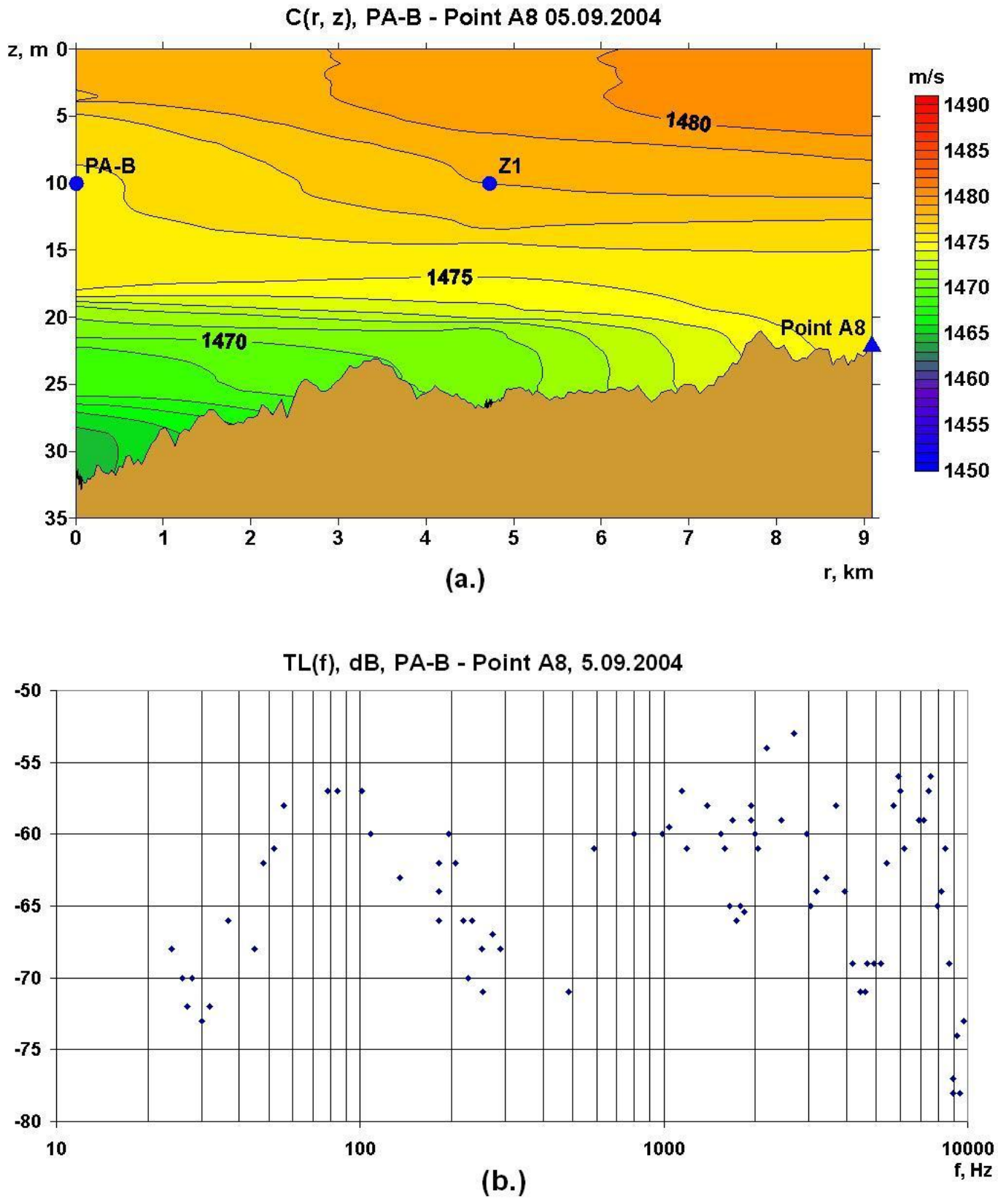

Figure 3.3 - PTL profile PTL1: (a) bathymetry and velocity C(z,r) along the profile as well as the source, receiver and intermediate hydrology locations. (b) Frequency dependent TL plot showing the results for the source location.

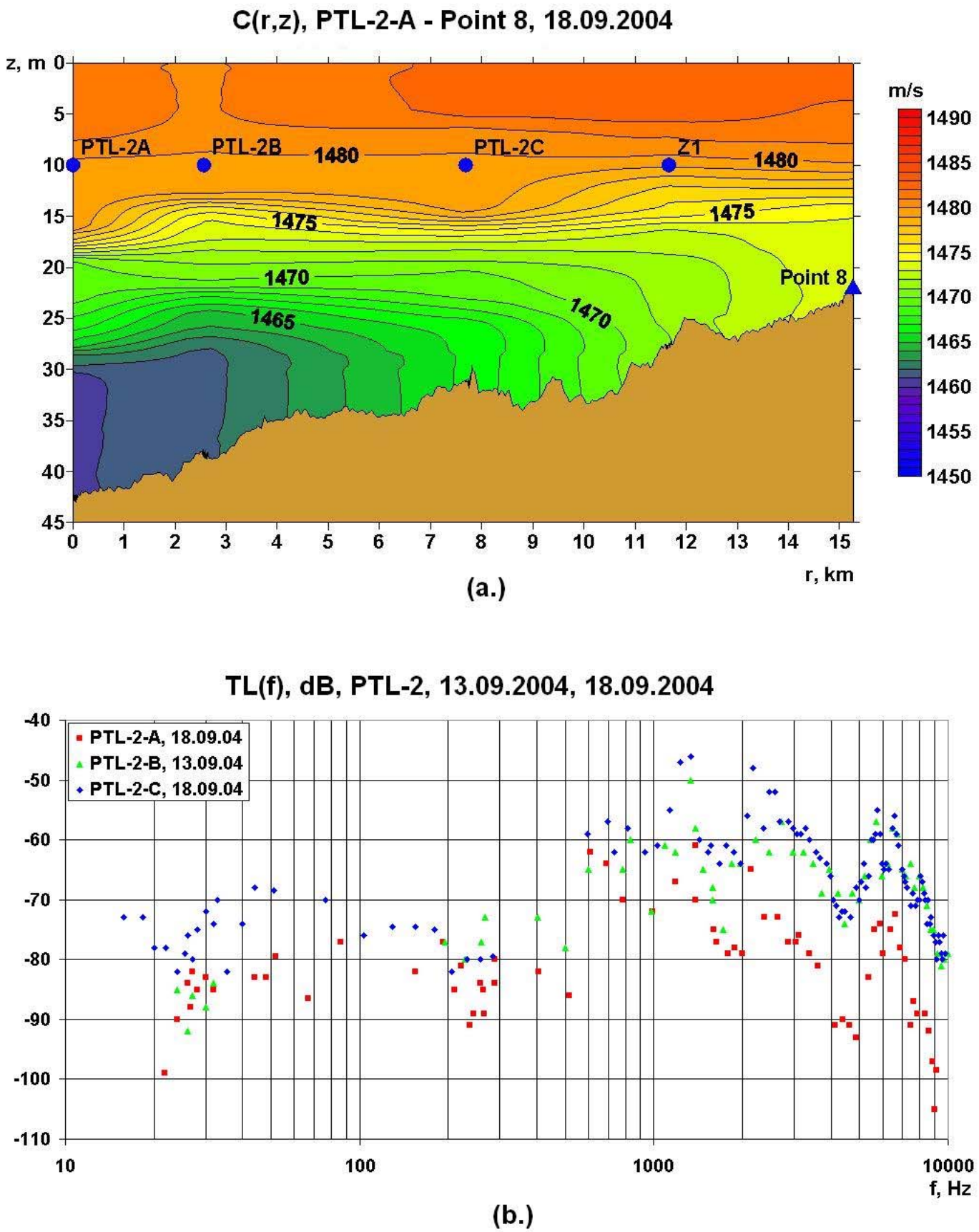

Figure 3.4 - PTL profile PTL2: (a) bathymetry and velocity C(z,r) along the profile as well as the source, receiver and intermediate hydrology locations. (b) Frequency dependent TL plot showing the results for all the source locations (in different colors).

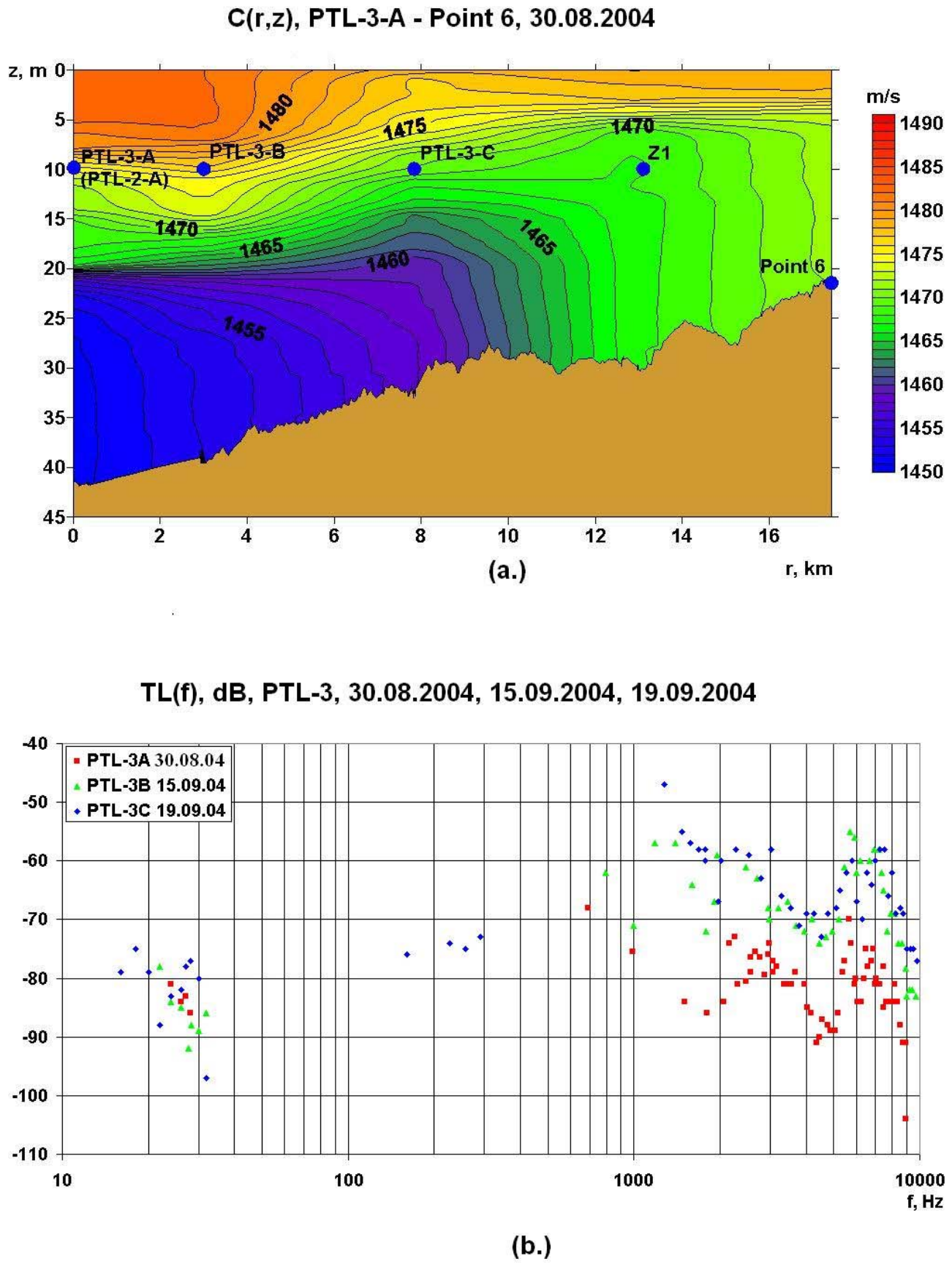

Figure 3.5 - PTL profile PTL3: (a) bathymetry and velocity C(z,r) along the profile as well as the source, receiver and intermediate hydrology locations. (b) Frequency dependent TL plot showing the results for all the source locations (in different colors).

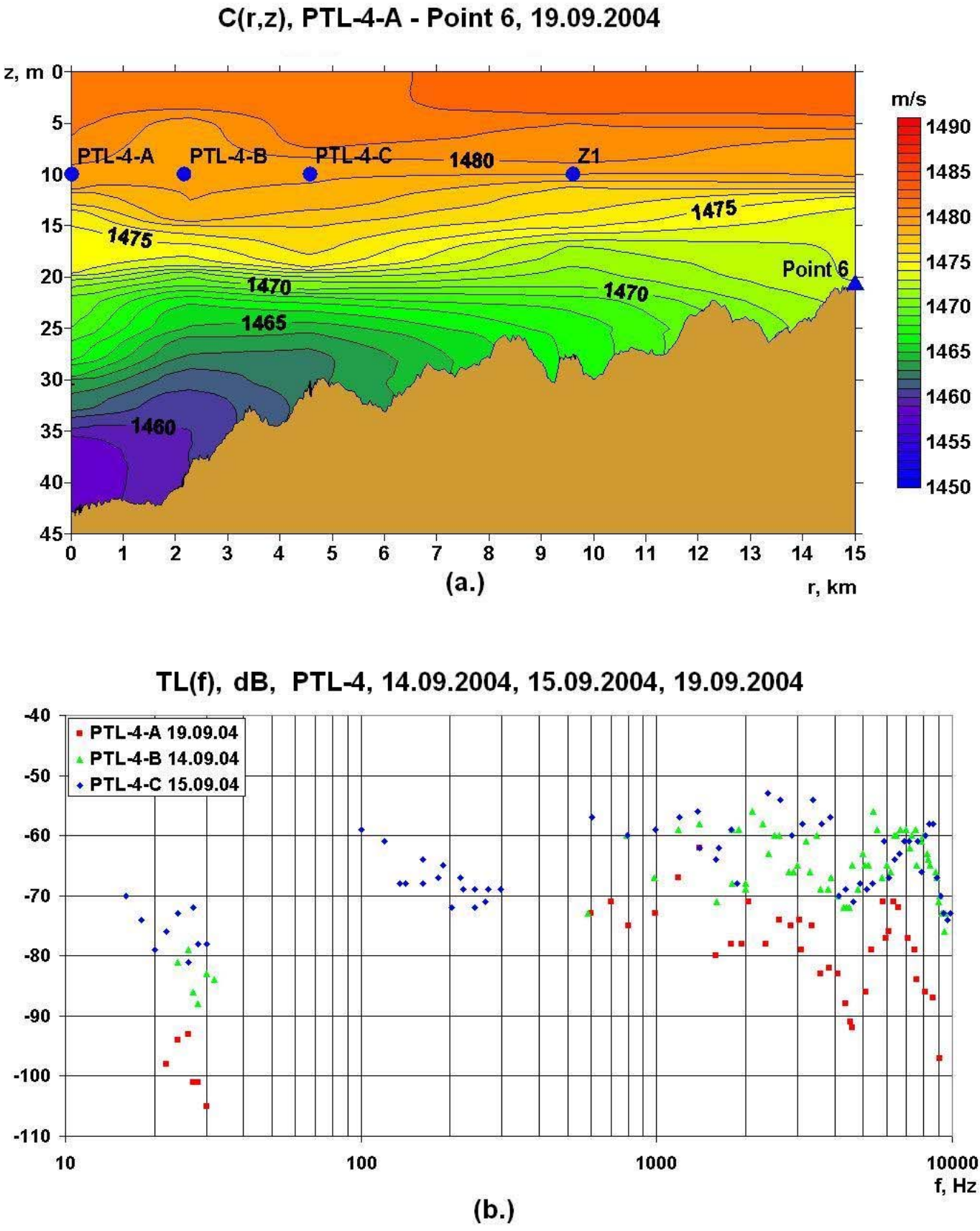

Figure 3.6 - PTL profile PTL4: (a) bathymetry and velocity C(z,r) along the profile as well as the source, receiver and intermediate hydrology locations. (b) Frequency dependent TL plot showing the results for all the source locations (in different colors).

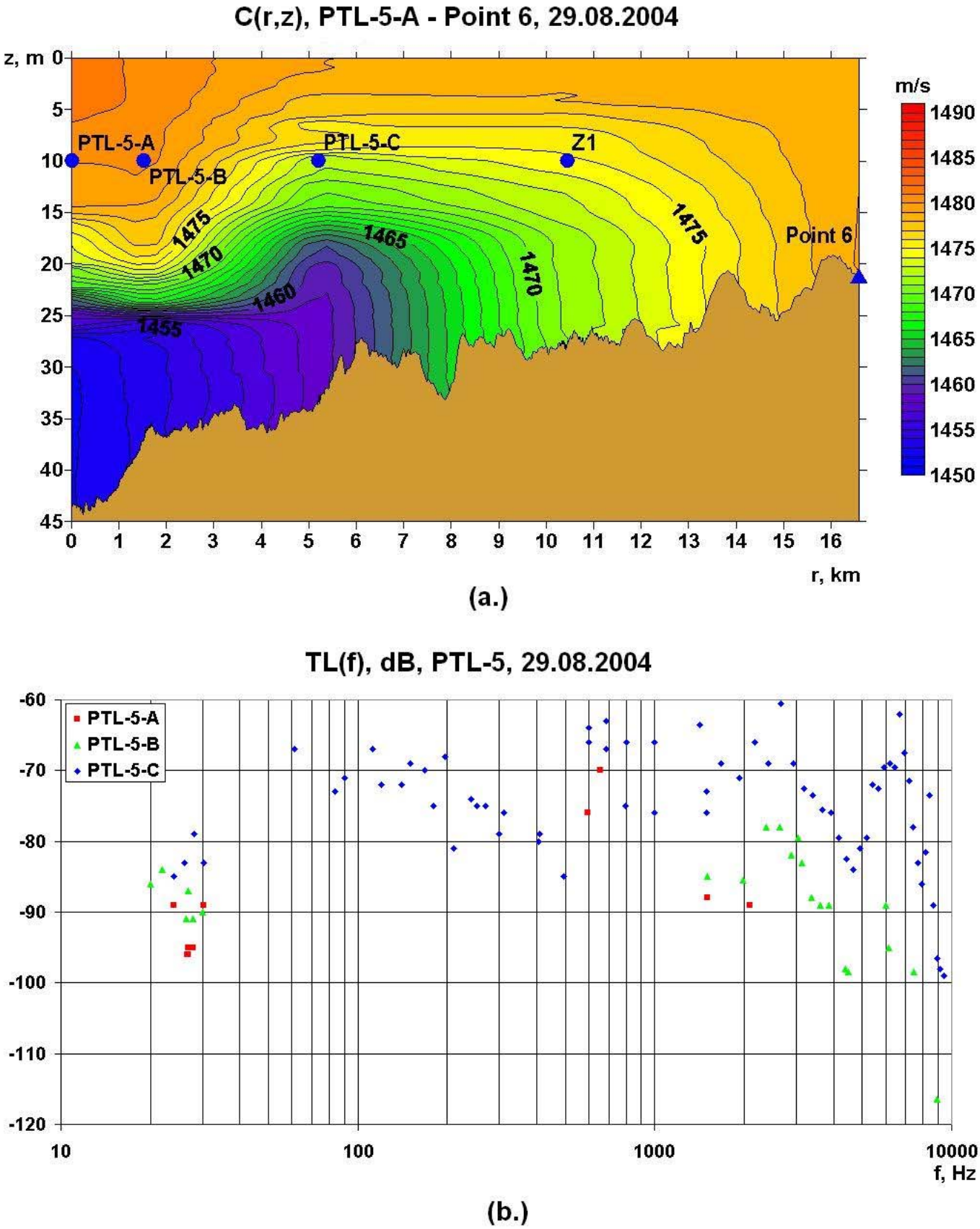

Figure 3.7 - PTL profile PTL5: (a) bathymetry and velocity C(z,r) along the profile as well as the source, receiver and intermediate hydrology locations. (b) Frequency dependent TL plot showing the results for all the source locations (in different colors).

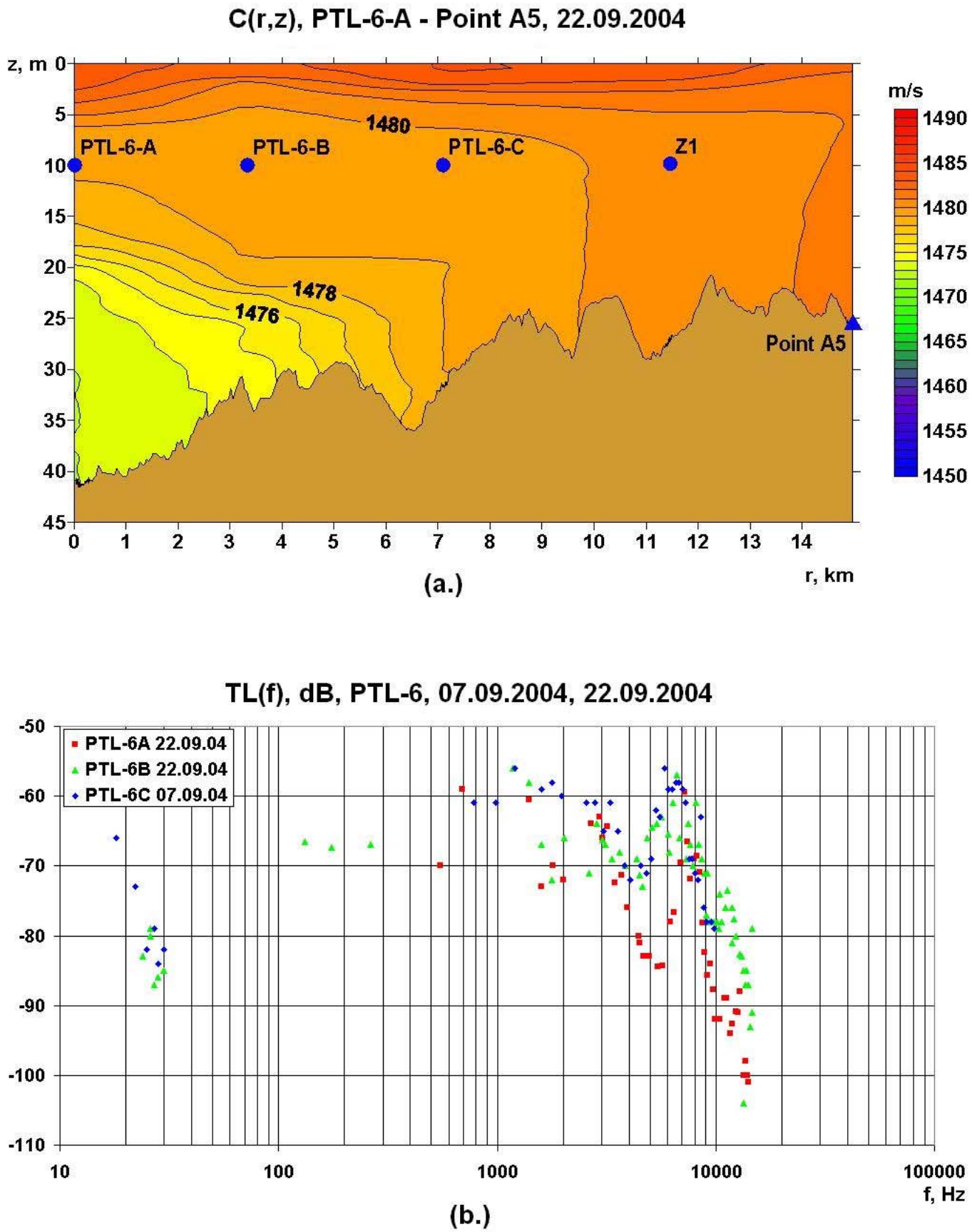

Figure 3.8 - PTL profile PTL6: (a) bathymetry and velocity C(z,r) along the profile as well as the source, receiver and intermediate hydrology locations. (b) Frequency dependent TL plot showing the results for all the source locations (in different colors).

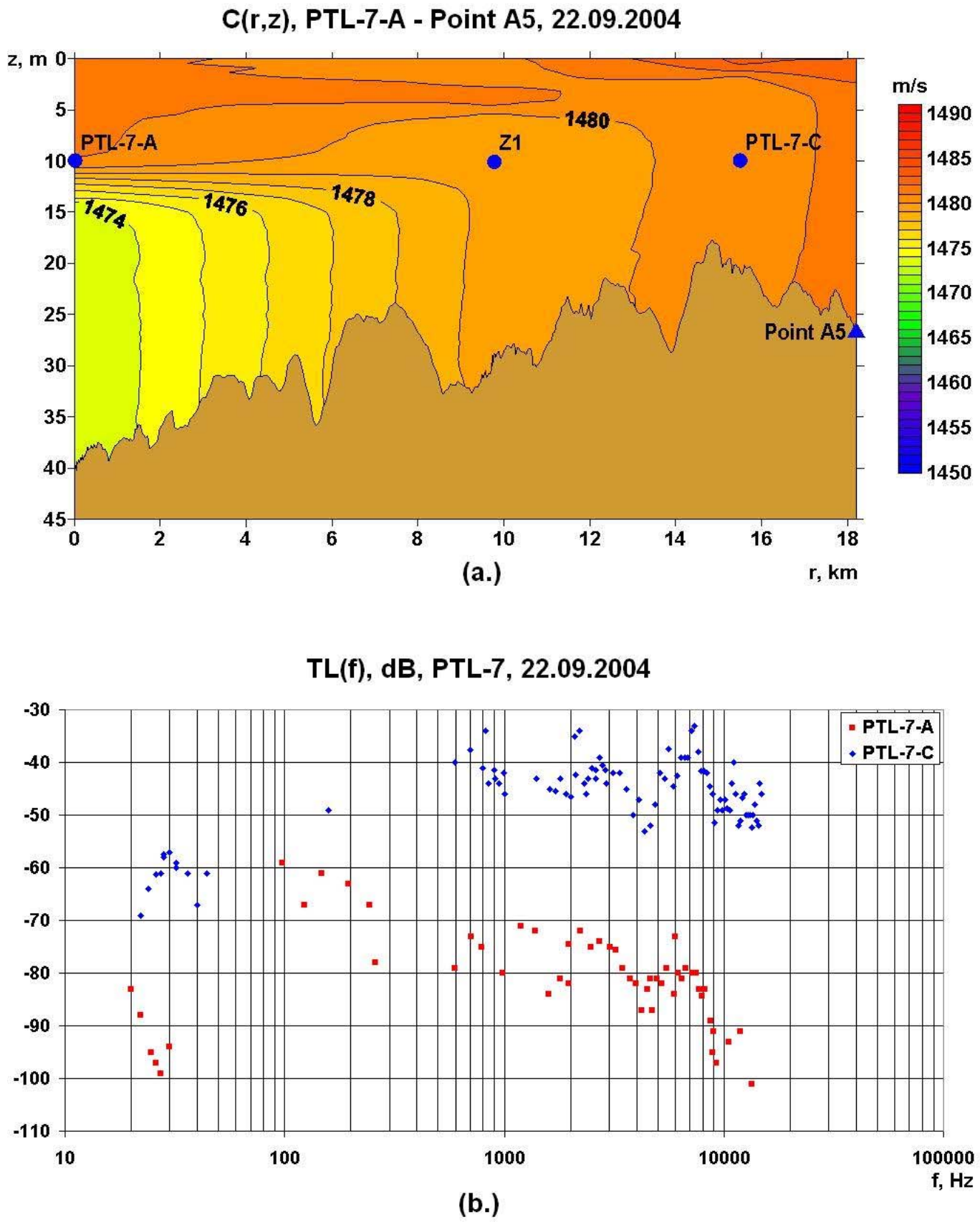

Figure 3.9 - PTL profile PTL7: (a) bathymetry and velocity C(z,r) along the profile as well as the source, receiver and intermediate hydrology locations. (b) Frequency dependent TL plot showing the results for all the source locations (in different colors).

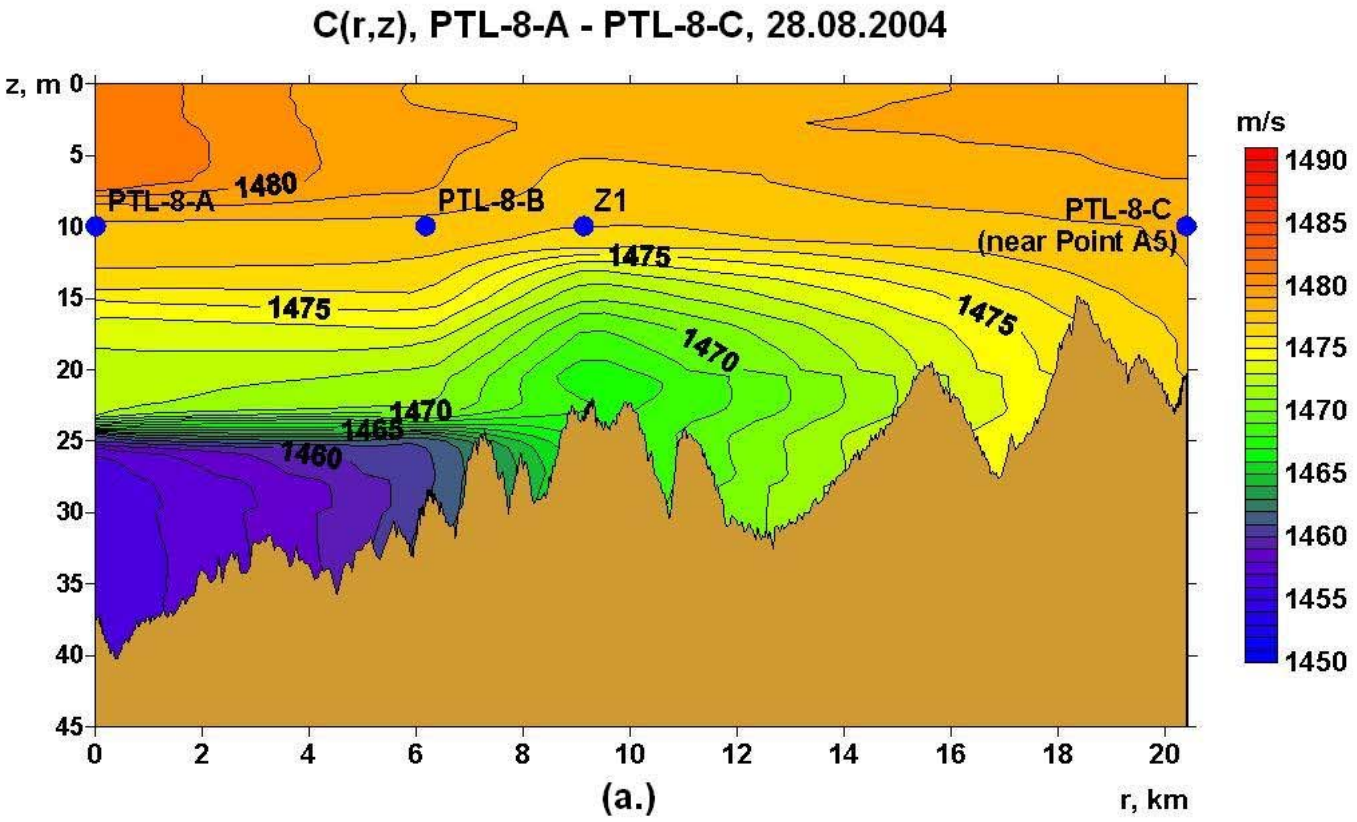

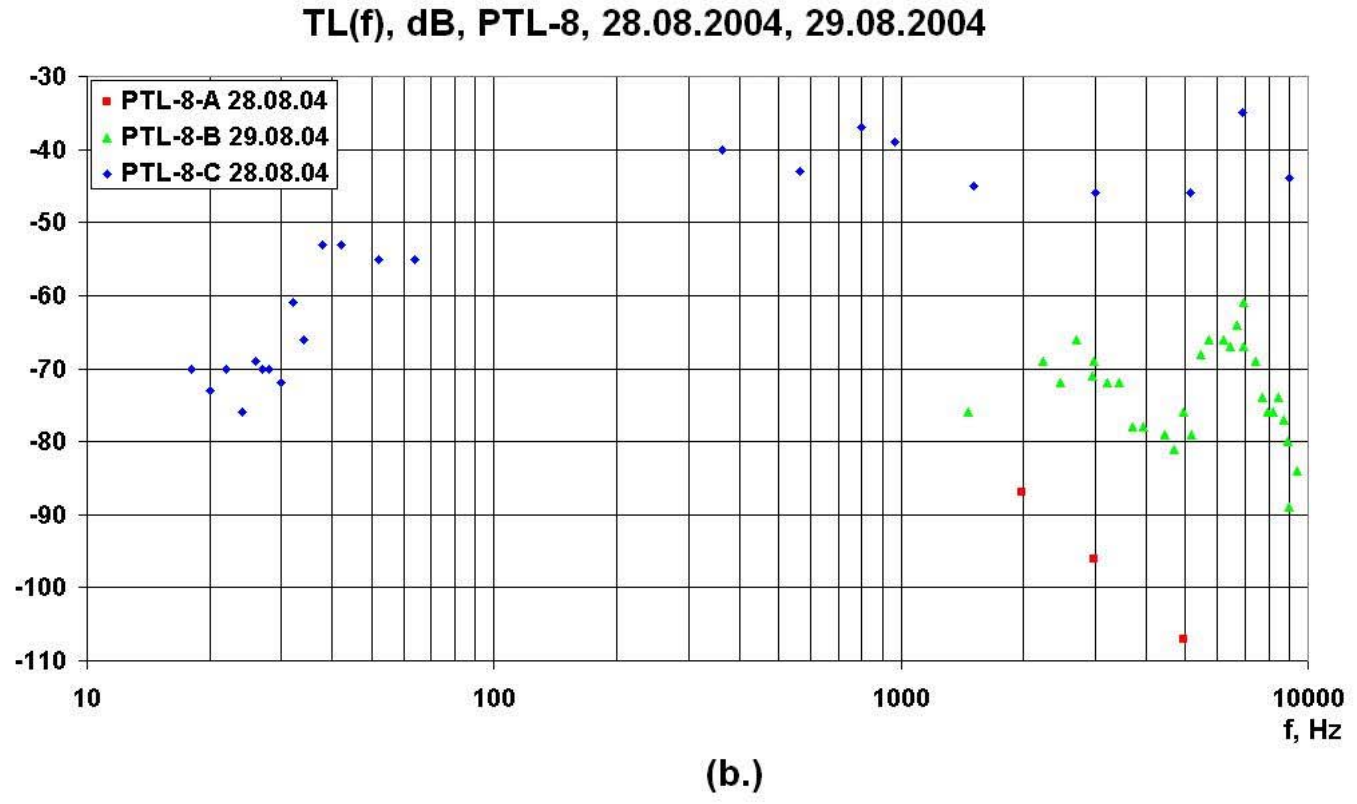

Figure 3.10 - PTL profile PTL8: (a) bathymetry and velocity C(z,r) along the profile as well as the source, receiver and intermediate hydrology locations. (b) Frequency dependent TL plot showing the results for all the source locations (in different colors).

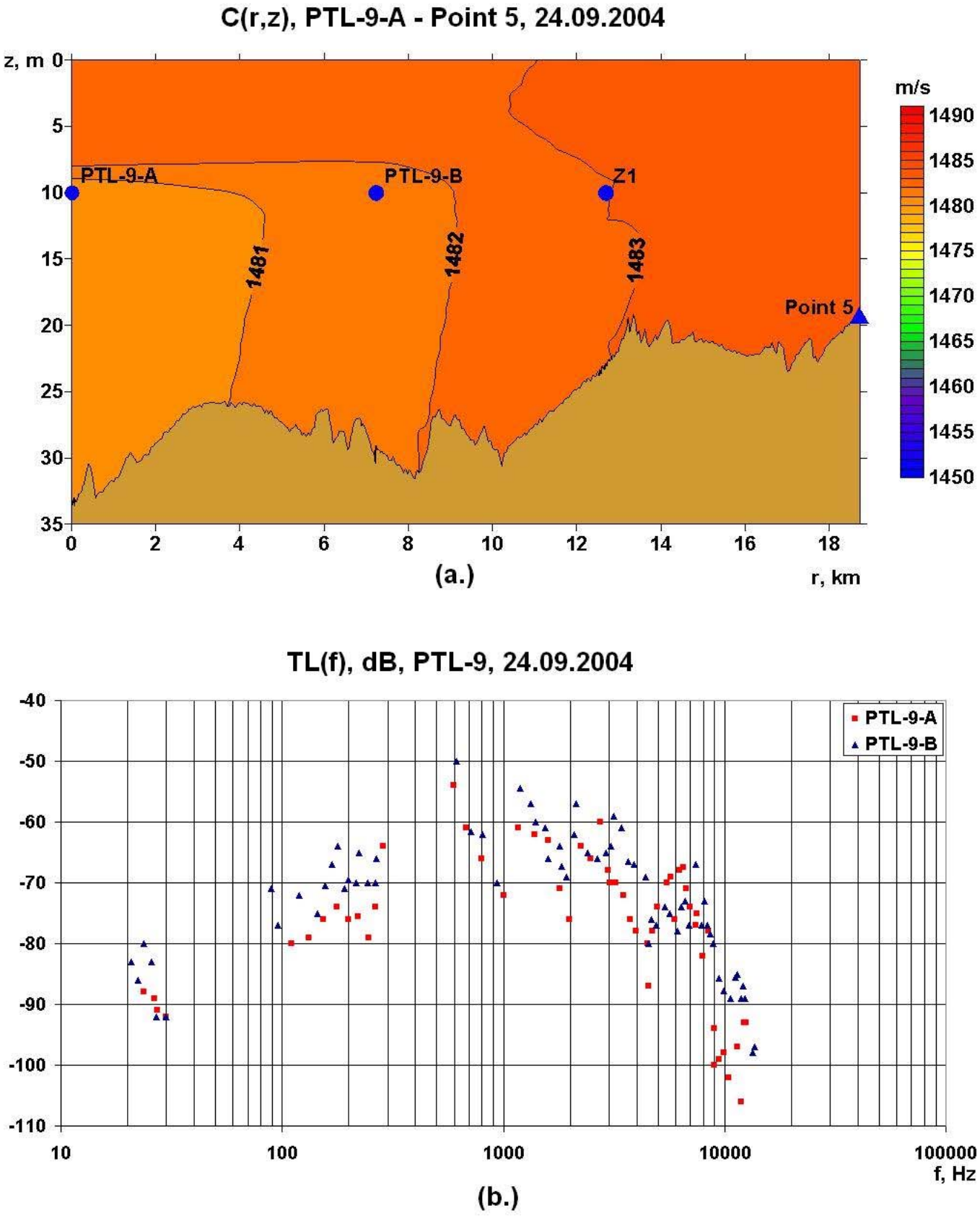

Figure 3.11 - PTL profile PTL9: (a) bathymetry and velocity C(z,r) along the profile as well as the source, receiver and intermediate hydrology locations. (b) Frequency dependent TL plot showing the results for all the source locations (in different colors).

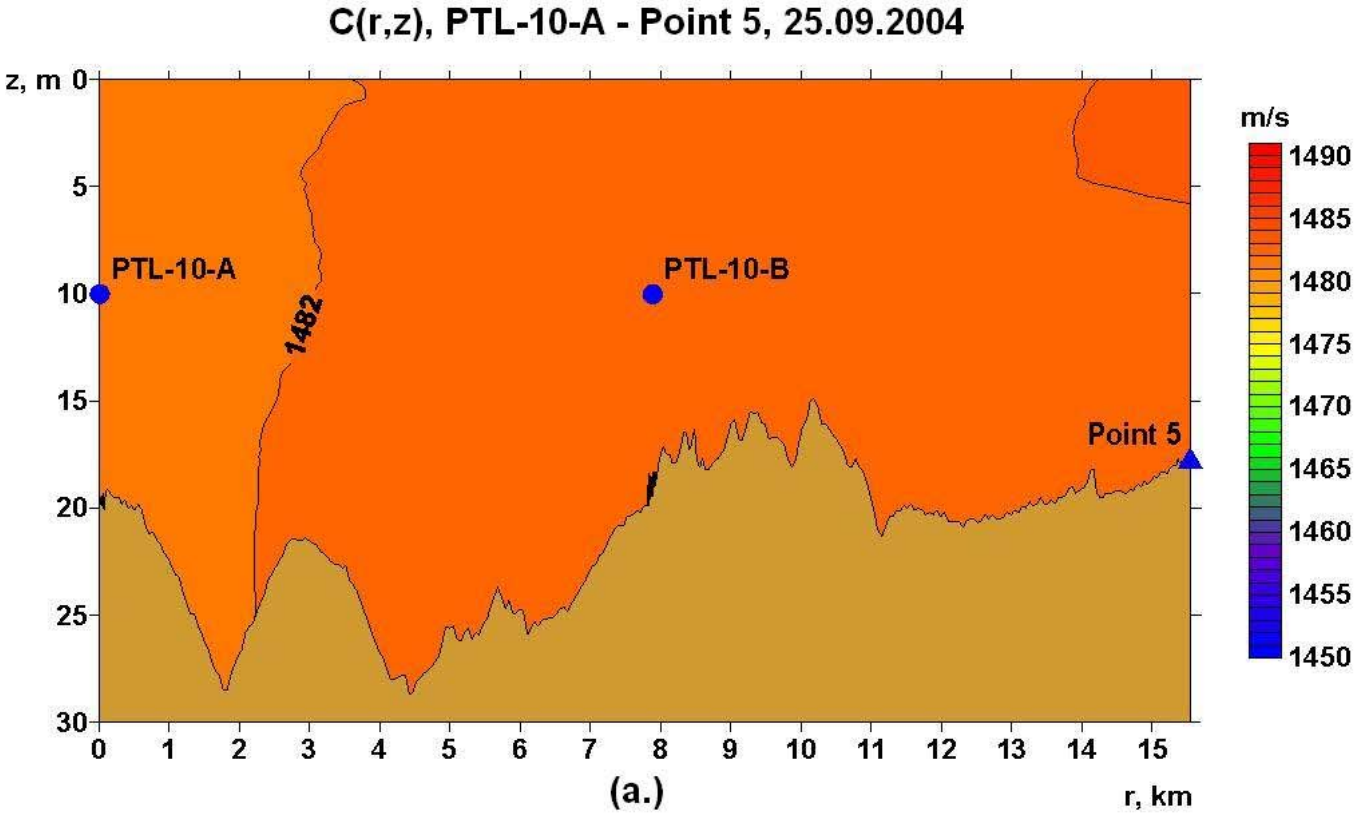

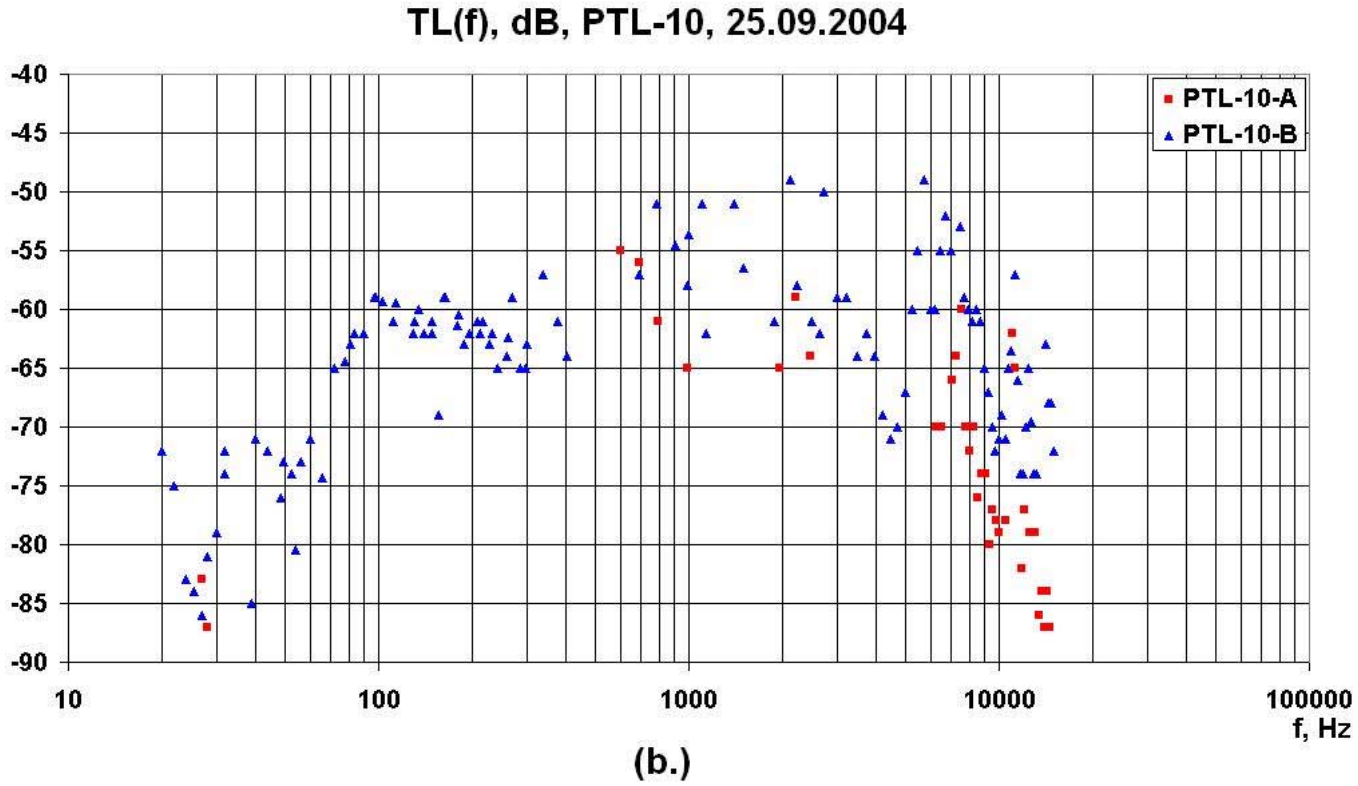

Figure 3.12 - PTL profile PTL10: (a) bathymetry and velocity C(z,r) along the profile as well as the source, receiver and intermediate hydrology locations. (b) Frequency dependent TL plot showing the results for all the source locations (in different colors).

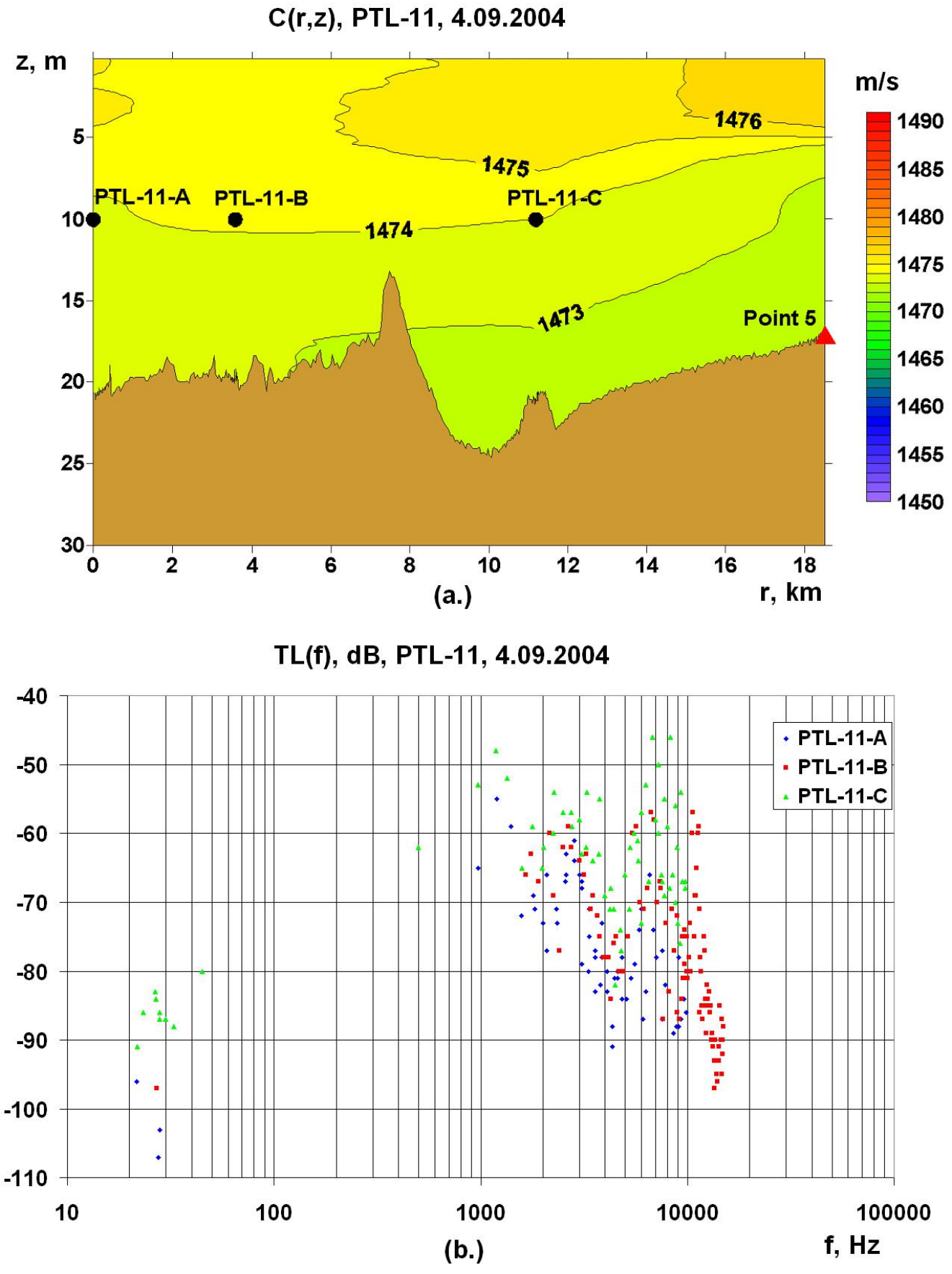

Figure 3.13 - PTL profile PTL11: (a) bathymetry and velocity C(z,r) along the profile as well as the source, receiver and intermediate hydrology locations. (b) Frequency dependent TL plot showing the results for all the source locations (in different colors).

Figure 3.14 shows the results of hydrological and acoustic measurements conducted on PTL profiles from locations PTL12-A and PTL13-A to the Orlan monitor station. Sound at frequencies from 25-35 Hz propagates from PTL-13A to Orlan with a TL of ~95 dB. The acoustic energy at frequencies of 25-32 Hz transmitted from location PTL-12A were below ambient noise levels at the Orlan monitor station. The TL between location PTL-12A and the Offshore feeding area cannot therefore be estimated.

Figure 3.15 shows the results of hydrological and acoustic measurements conducted on PTL profiles from locations PTL12-A and PTL13-A to the Piltun-S monitor station. These profiles are relatively shallow and oriented sub-parallel to the coast. The TL along these profiles for frequencies of 24-32 Hz again cannot be estimated.

3.4 Analysis of TL from Orlan Platform to the Piltun and Offshore Feeding Areas

Figures 3.16 and 3.17 show TL profiles from the Orlan platform location. Figure 3.16 displays the TL profile (TLP-2) that extends from the Orlan platform to the Offshore feeding area (Orlan and Arkutun-Dagi monitor stations). Figure 3.16(a) is a schematic map showing the layout of profile TLP-2. There are six source locations (A, B, C, E, F and G) along the profile. The transducers were operated at each location while *Akademik Oparin* was drifting; each location is marked with two asterisks corresponding to initial and final position of the vessel. At the Orlan platform location and source locations TLP2-D and TLP2-H the *Akademik Oparin* was anchored. Figure 3.16(b) shows the bathymetric profile and velocity distribution C(z,r) constructed from hydrologic measurements acquired on 27 September. Figure 3.16(c) gives the frequency dependent TL results for TLP-2.

Figure 3.17 displays the TL profile (TLP-6) that extends from the Orlan platform to southern edge of the Piltun feeding area (Piltun-S monitor station and acoustic station A4). Again the acoustic energy at frequencies of 25-35 Hz propagating from the Orlan platform to the southern edge of the inshore feeding area is below ambient noise and the TL cannot be estimated.

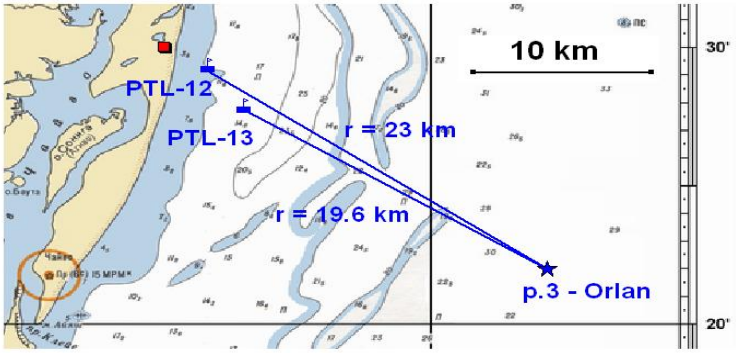

(a.)

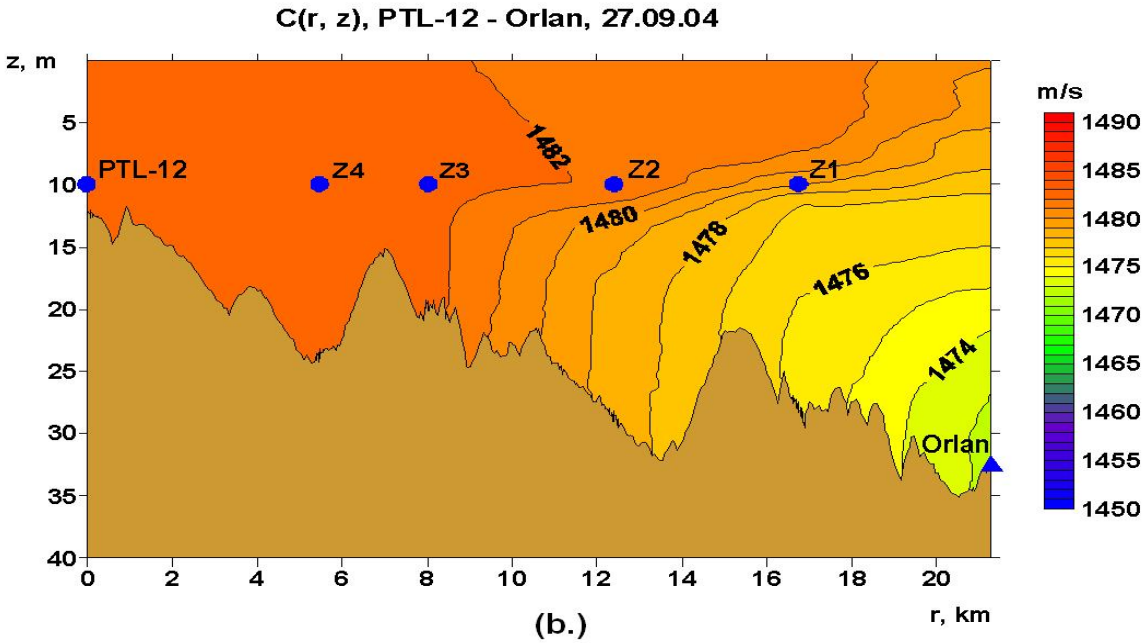

(b.)

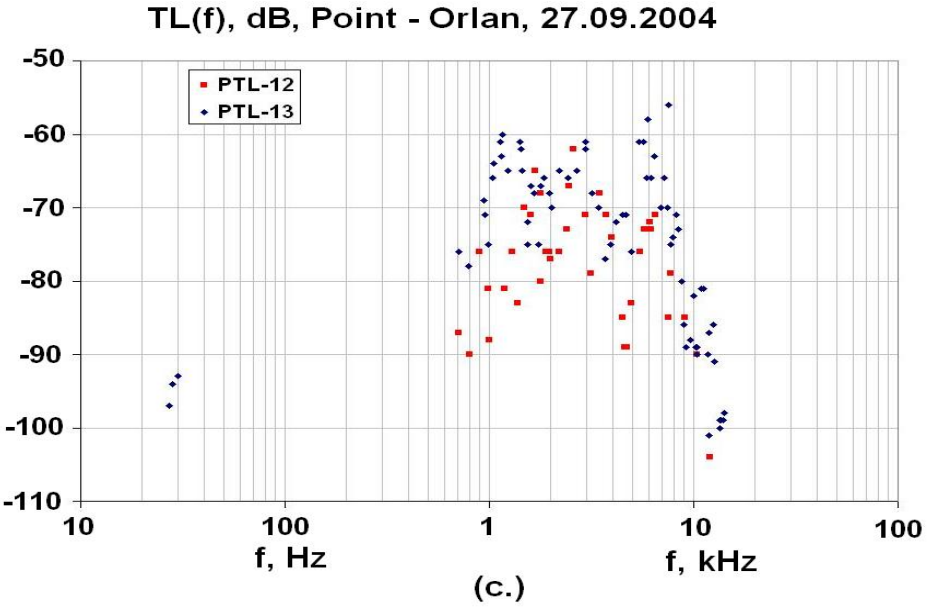

(c.)

Figure 3.14 - PTL profiles from locations PTL12-A and PTL13-A to the Orlan monitor station. (a) Schematic map showing the experimental layout (b) bathymetry and velocity C(z,r) along the profile from PTL12-A as well as the source, receiver and intermediate hydrology locations. (c) Frequency dependent TL plot showing the results for both source locations.

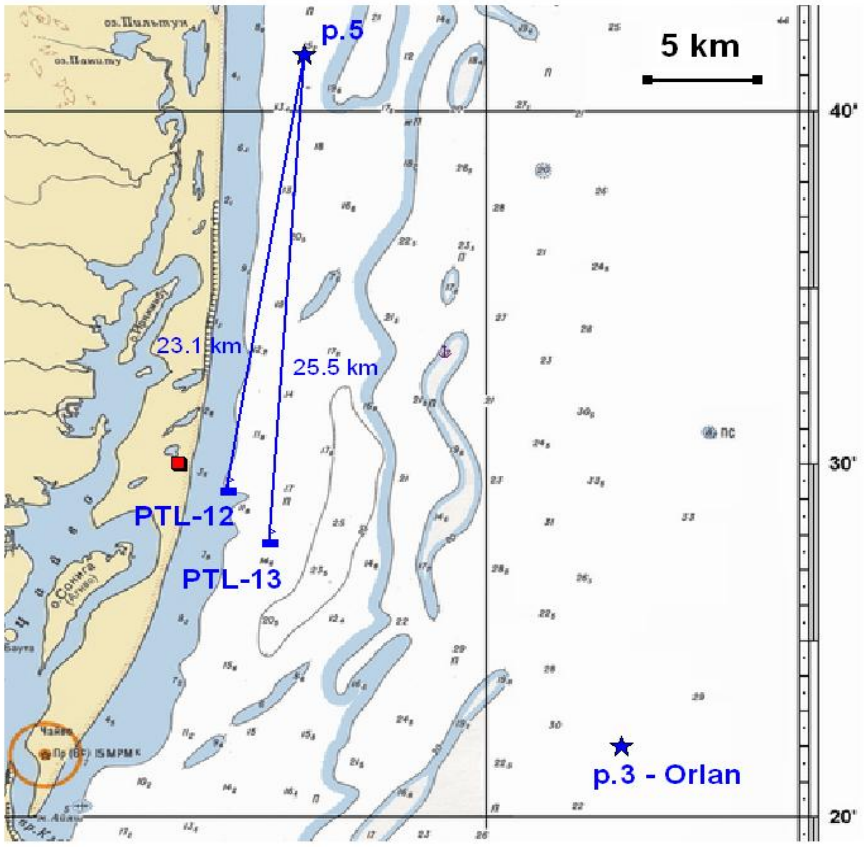

(a.)

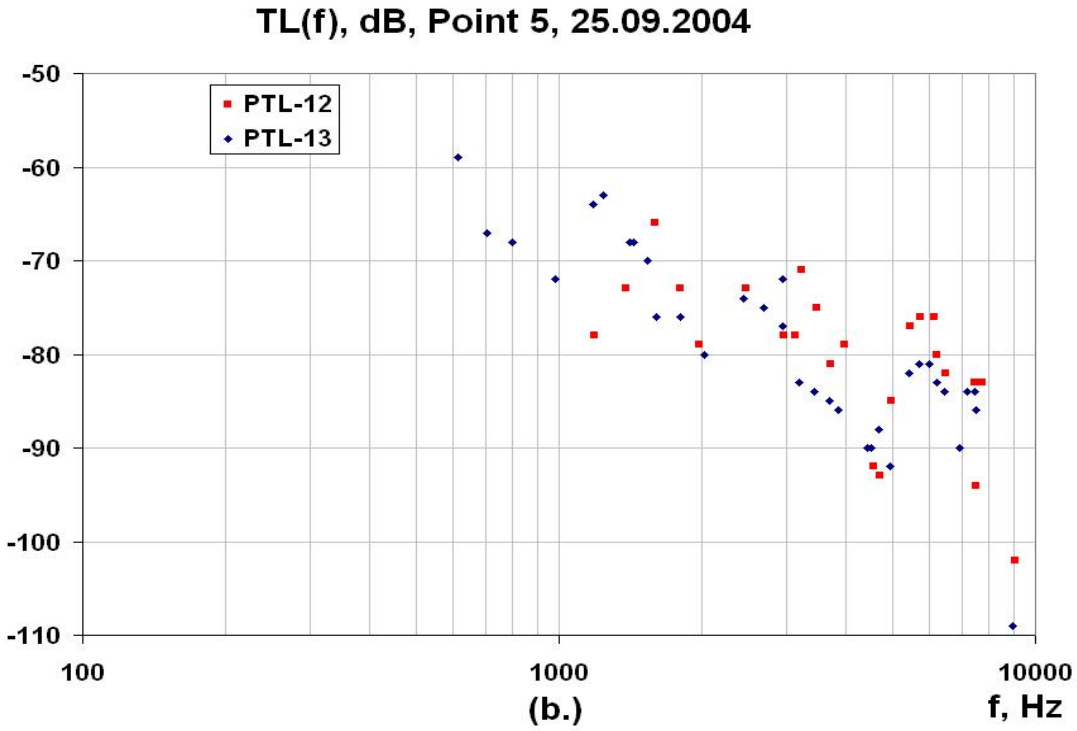

(b.)

Figure 3.15 - PTL profiles from locations PTL12-A and PTL13-A to the Piltun-S monitor station. (a) Schematic map showing the experimental layout (b) Frequency dependent TL plot showing the results for both source locations.

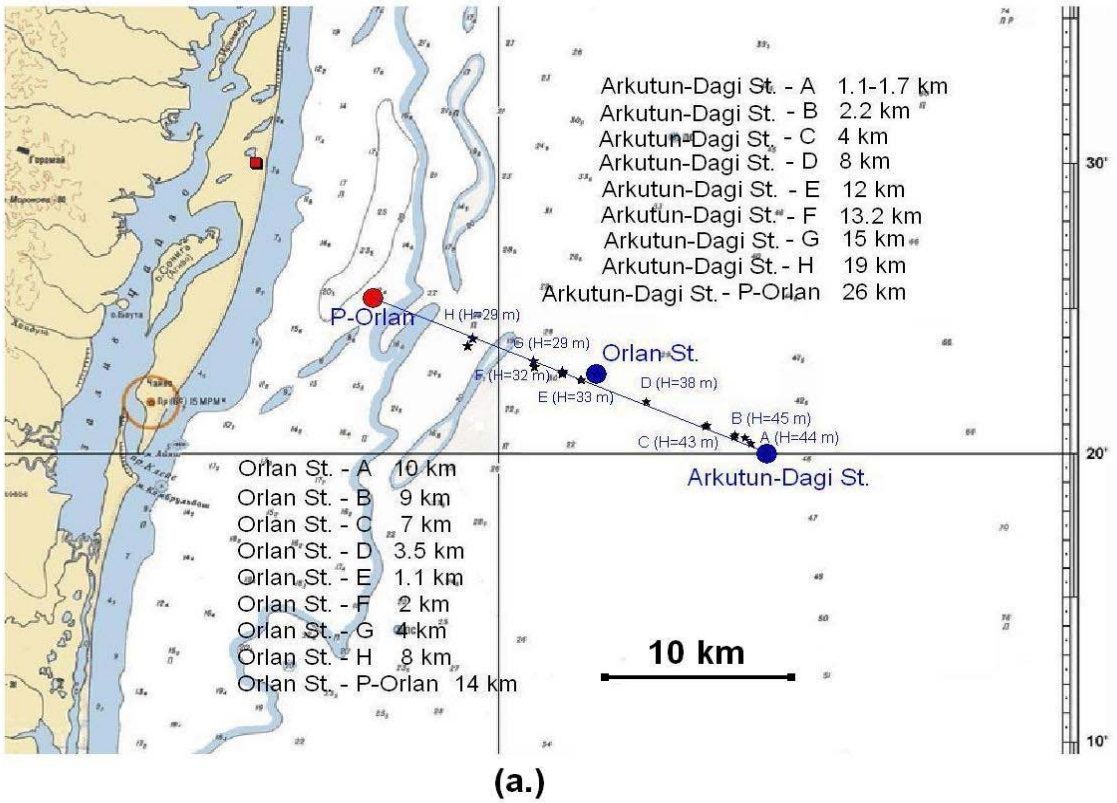

(a.)

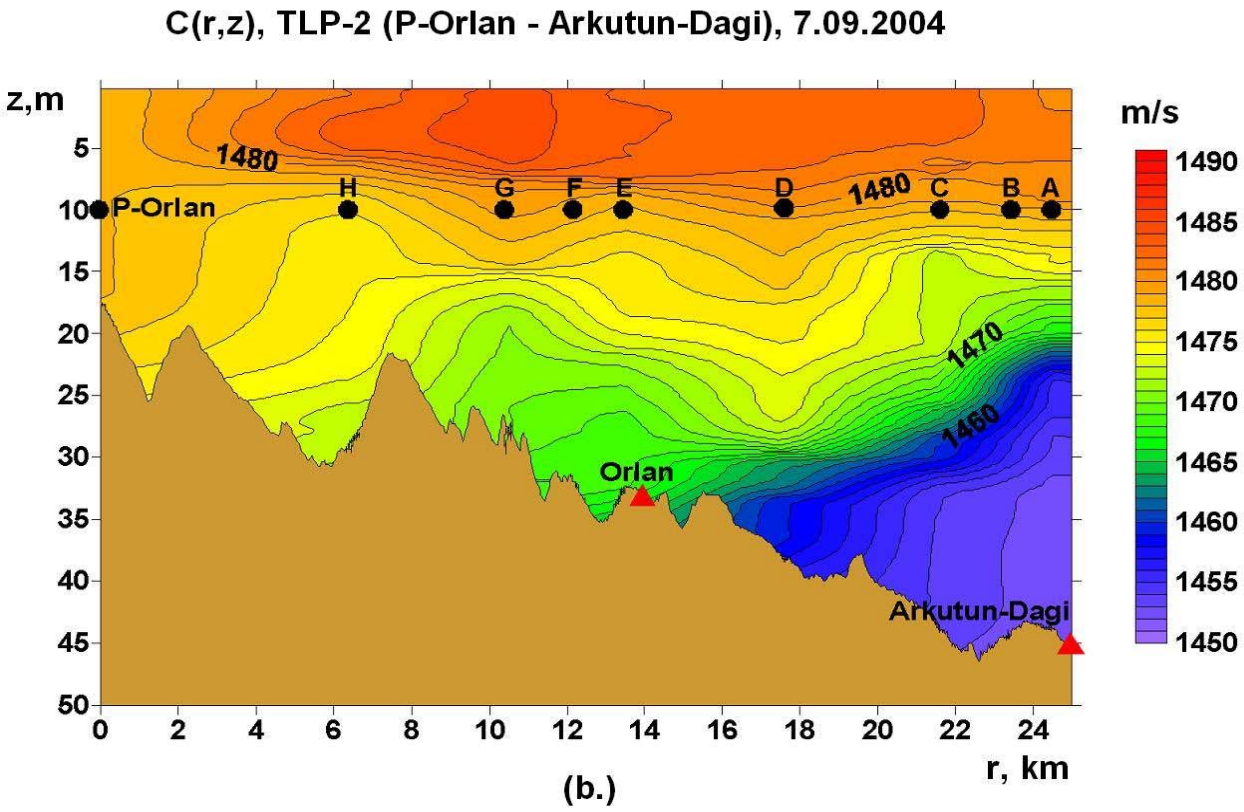

(b.)

Figure 3.16 - TL profiles TLP-2 from the Orlan platform location to the Orlan and Arkutun-Dagi monitor station. (a) Schematic map showing the experimental layout (b) bathymetry and velocity C(z,r) along the profile as well as the source, receiver and intermediate hydrology locations.

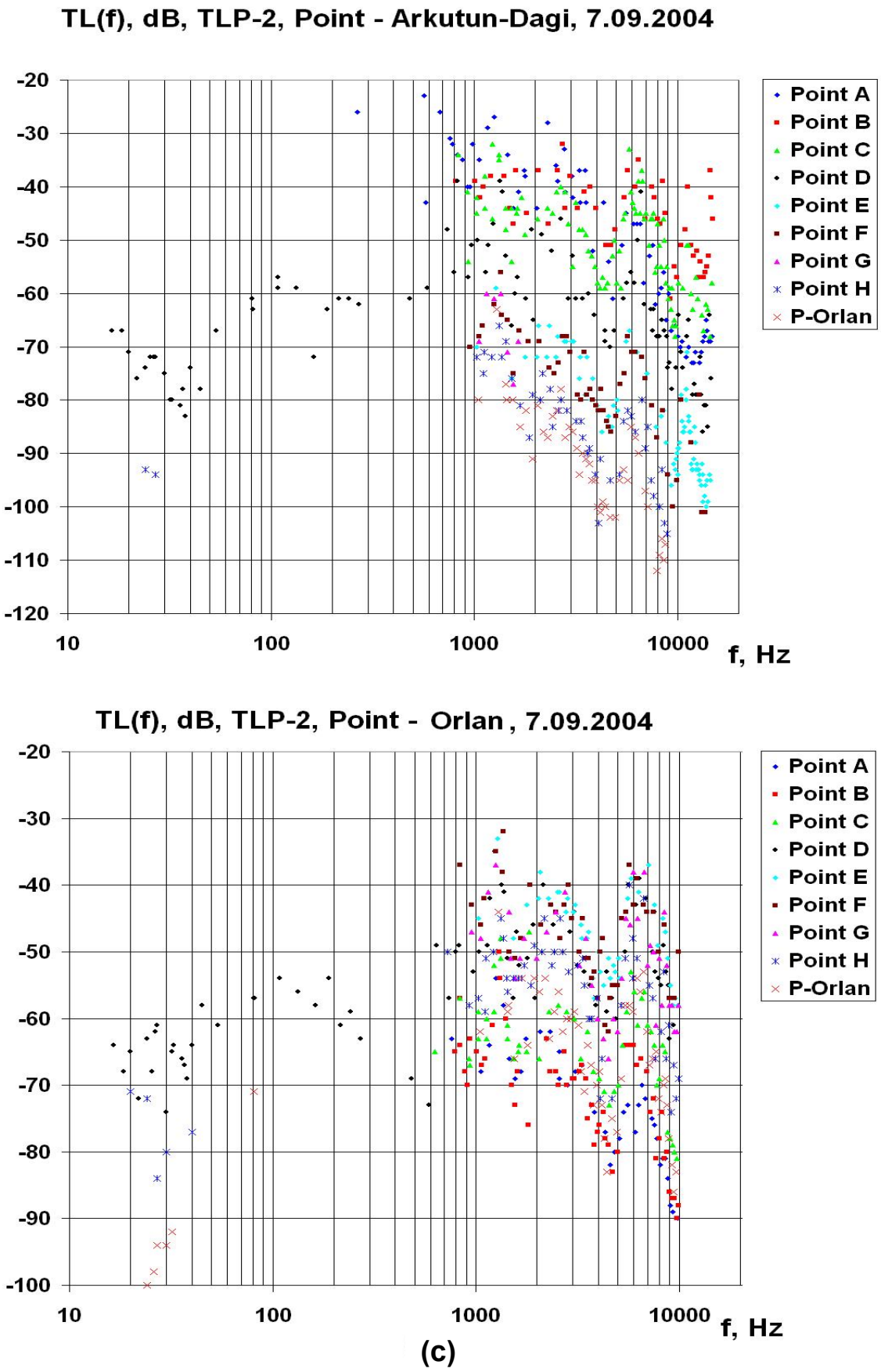

Figure 3.16 - TL profiles TLP-2 from the Orlan platform location to the Orlan and Arkutun-Dagi monitor station. (c) Frequency dependent TL plot showing the results for both receiver locations.

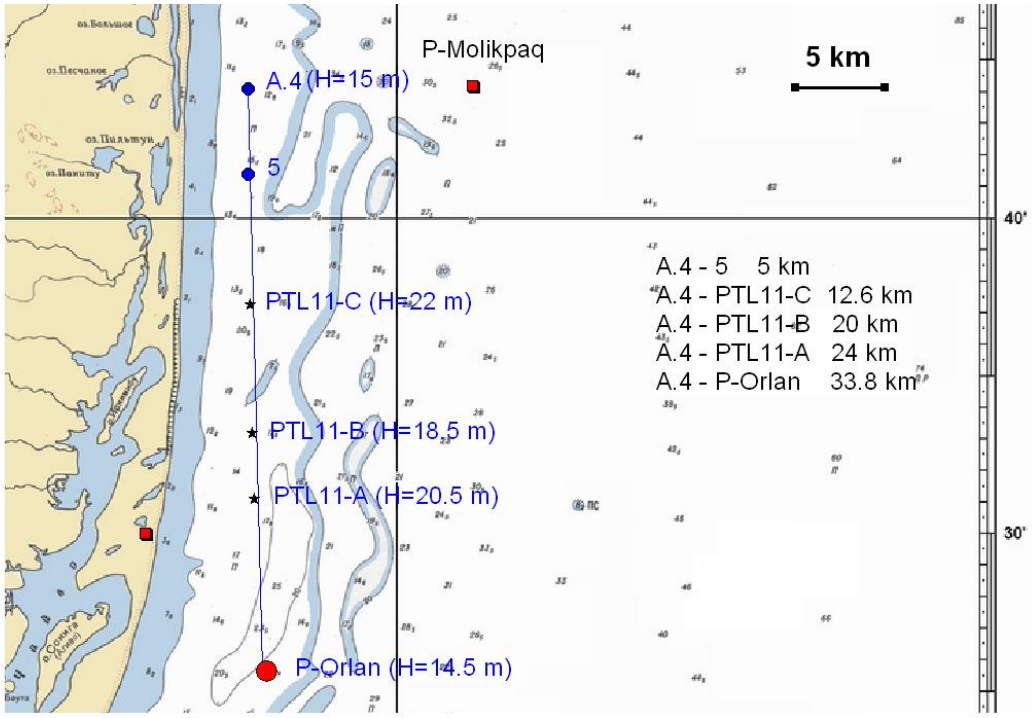

(a.)

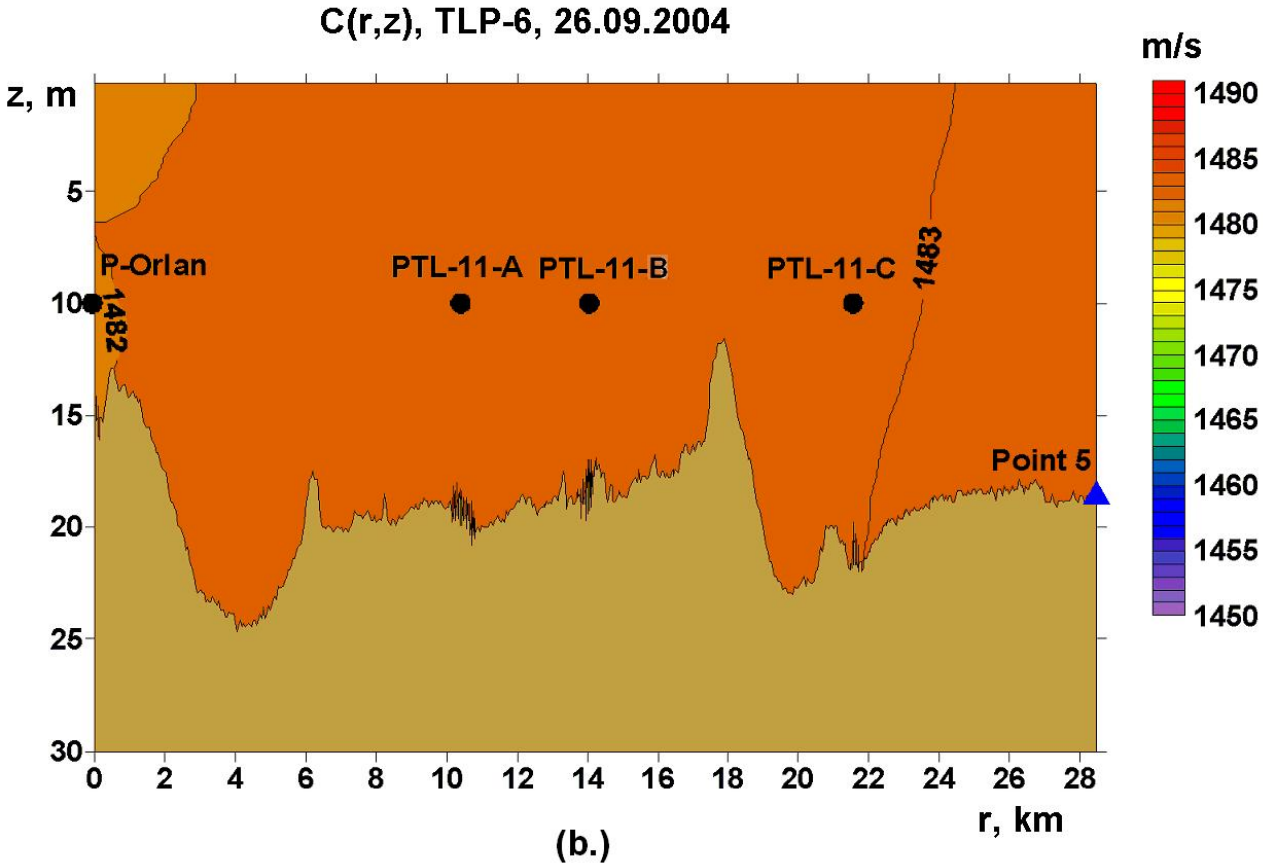

(b.)

Figure 3.17 - TL profiles TLP-6 from the Orlan platform location to the Piltun-S monitor station. (a) Schematic map showing the experimental layout (b) bathymetry and velocity C(z,r) along the profile as well as the source, receiver and intermediate hydrology locations.

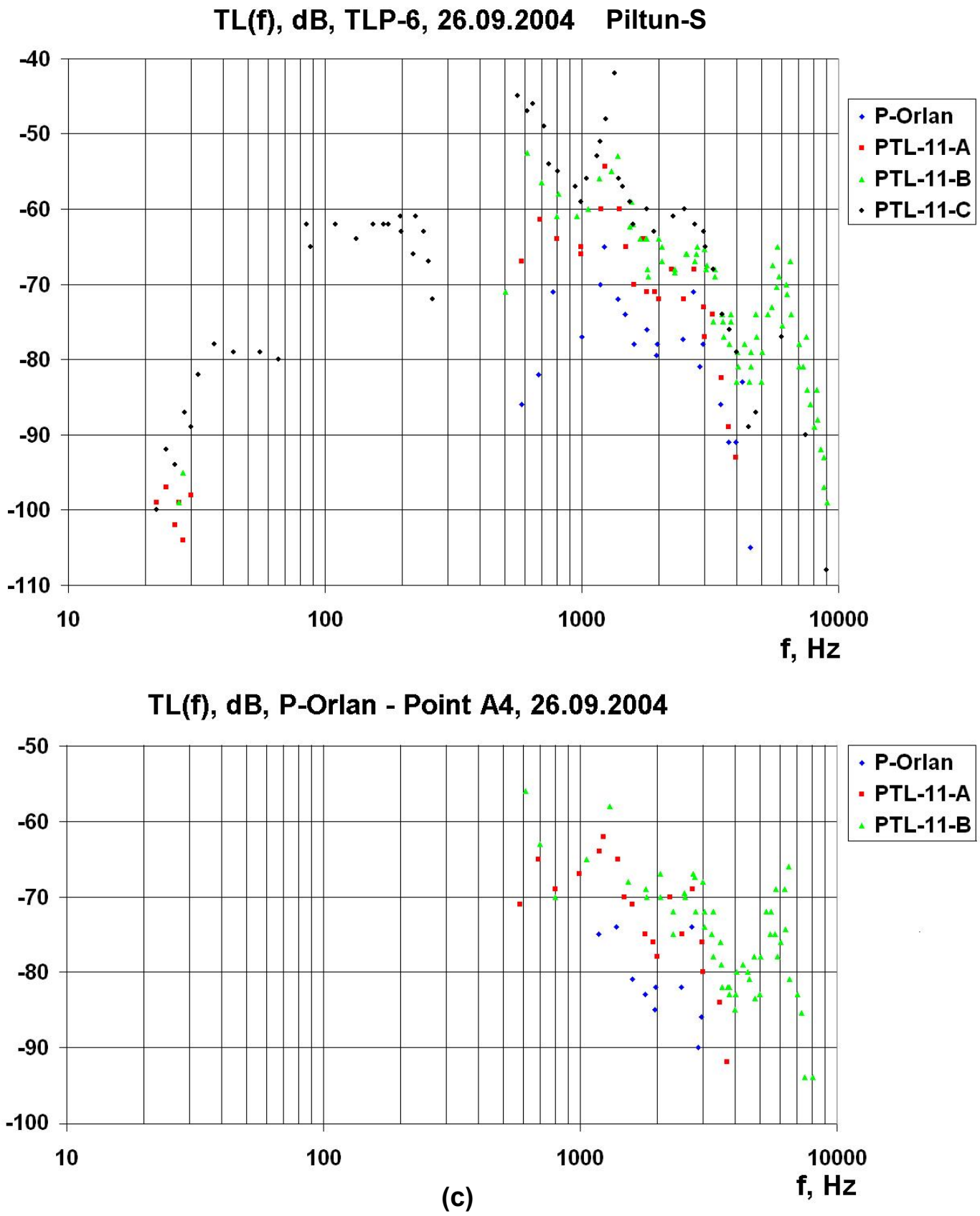

Figure 3.17 - TL profiles TLP-6 from the Orlan platform location to the Piltun-S monitor station and the A4 acoustic station. (c) Frequency dependent TL plot showing the results for both receiver locations.

For some of the profiles to the Offshore feeding area, dynamic range considerations prevented the experimental estimation of TL for low frequencies. Numerical models were therefore used to attempt to estimate the low frequency TL for these profiles. These numerical models used the bathymetric, hydrologic and acoustic data available for the profile. Figure 3.18 shows the geometry of the waveguide and the parameters used for the numerical modeling along six profiles. The profiles are from the PTL-12A, PTL13-A and Orlan locations to the Orlan and Piltun-S monitor stations. The source and receiver locations in the model are approximately equal to the transducer and AUAR locations for the experiments. The bathymetric profile in the model is a smoothed version of the actual bathymetry along the profile; the acoustic velocity distribution was derived from the hydrologic data[25].

The theoretical TL values were estimated using the program MOATL[26] [Miller et.al., 1980] for the three-layer model with liquid sediment layer and elastic basement pictured in Figure 3.18. Figure 3.19 presents the results of this numerical modeling for these model waveguides. Figure 3.19 shows that the theoretical TL values for frequencies of 25-30 Hz propagating in the model waveguide from the Orlan platform to the Orlan monitor station agree with the experimental values from profile TLP-2 (Figure 3.16(c)). For relatively long shallow profiles oriented approximately parallel to the coast the theoretical TL values at frequencies of 20-30 Hz are even lower (-155 dB).

[25] The profiles oriented towards the southern edge of the Piltun feeding area (Piltun-S monitor station) correspond to actual experiments conducted on the 25 and 26 September. The hydrology was virtually homogeneous during the experiments. The profiles oriented towards the Offshore feeding area correspond to experiments conducted in different hydrologic conditions. The profile from Orlan to the Orlan monitor station (TLP-2) was acquired on 7 September; the profiles from PTL13-A and PTL12-A to the Orlan monitor station were acquired on the 27 September.

[26] MOATL is a mode theory approximation of acoustic propagation with non-interacting modes (adiabatic).

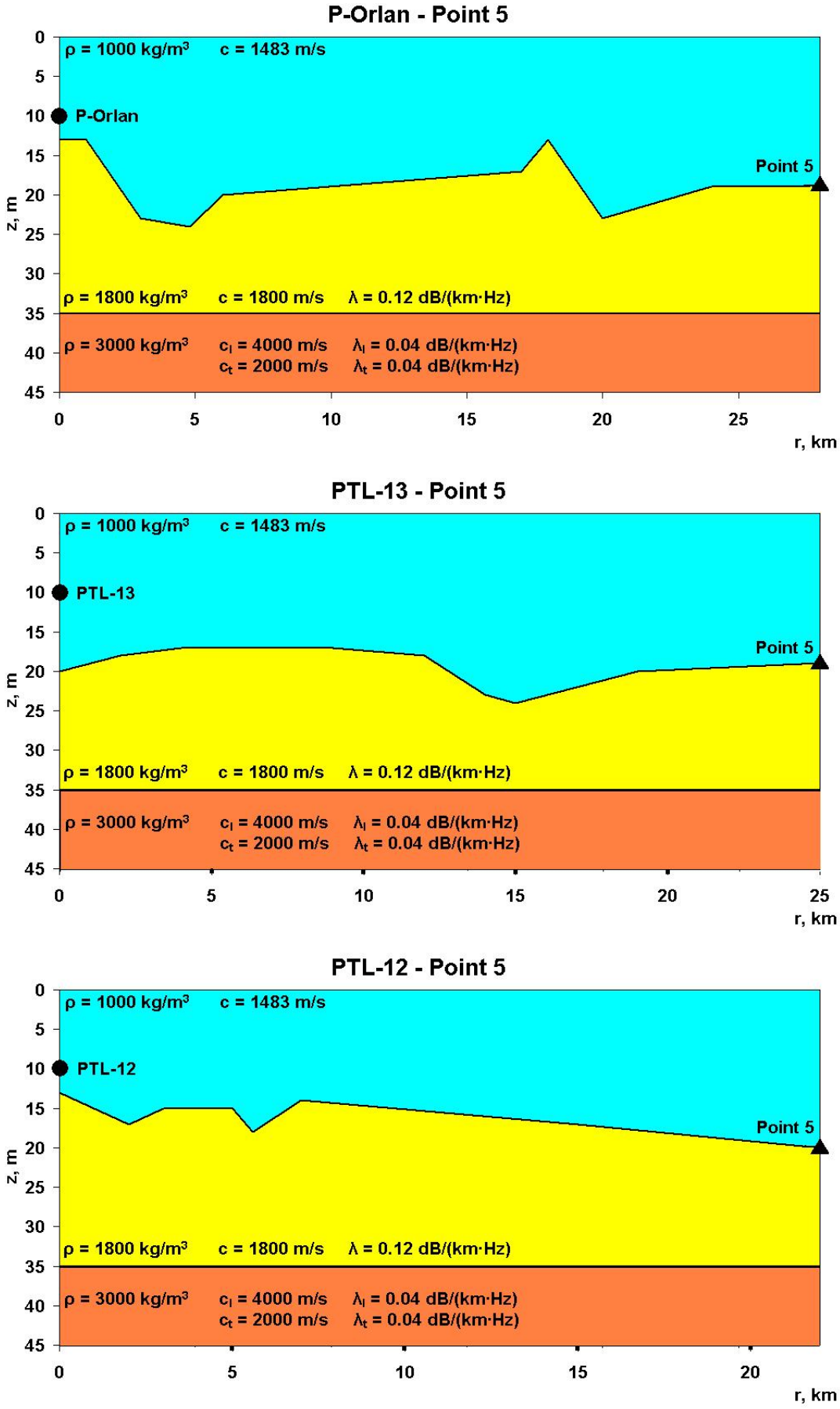

Figure 3.18 - Models of the acoustic waveguides used for the numerical modeling. Profiles from the PTL-12A, PTL13-A and Orlan locations to the Piltun-S monitor station.

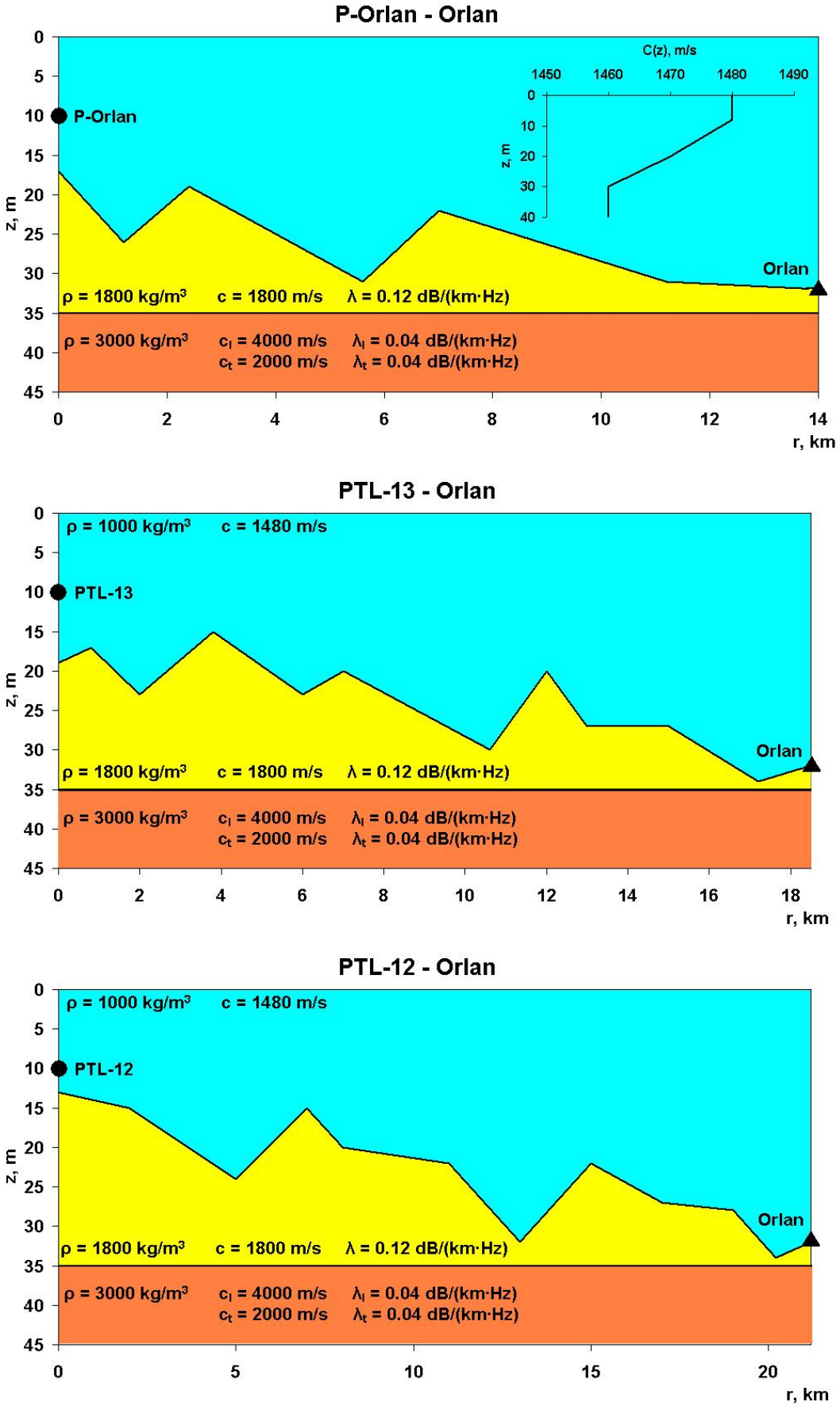

Figure 3.18 - Models of the acoustic waveguides used for the numerical modeling. Profiles from the PTL-12A. PTL13-A and Orlan locations to the Orlan monitor station.

3.5 Analysis of TL from the Odoptu License to the Piltun Feeding Area

Figure 3.20 shows acoustic profile TLP-14. This profile was oriented east-west, with seven source locations being acquired (TLP14-A, -B, -C, -D, -E, -F, and -G). The data was recorded on the Odoptu-S-10 and Odoptu-S-20 monitor stations. Acoustic signals were generated by the transducers deployed at 8 m depth from the *Academik Oparin*. Unfortunately the gains on the AUARs were selected to optimize the recording of ambient noise and the acoustic signature of the *Academik Oparin* overdrove the input voltage of the recorder while the near source locations (TLP14-A, -B and -C) were being acquired (Figure 3.20(a)). Figure 3.15(c) therefore presents only the TL results from locations TLP14- D, -E, -F, and -G.

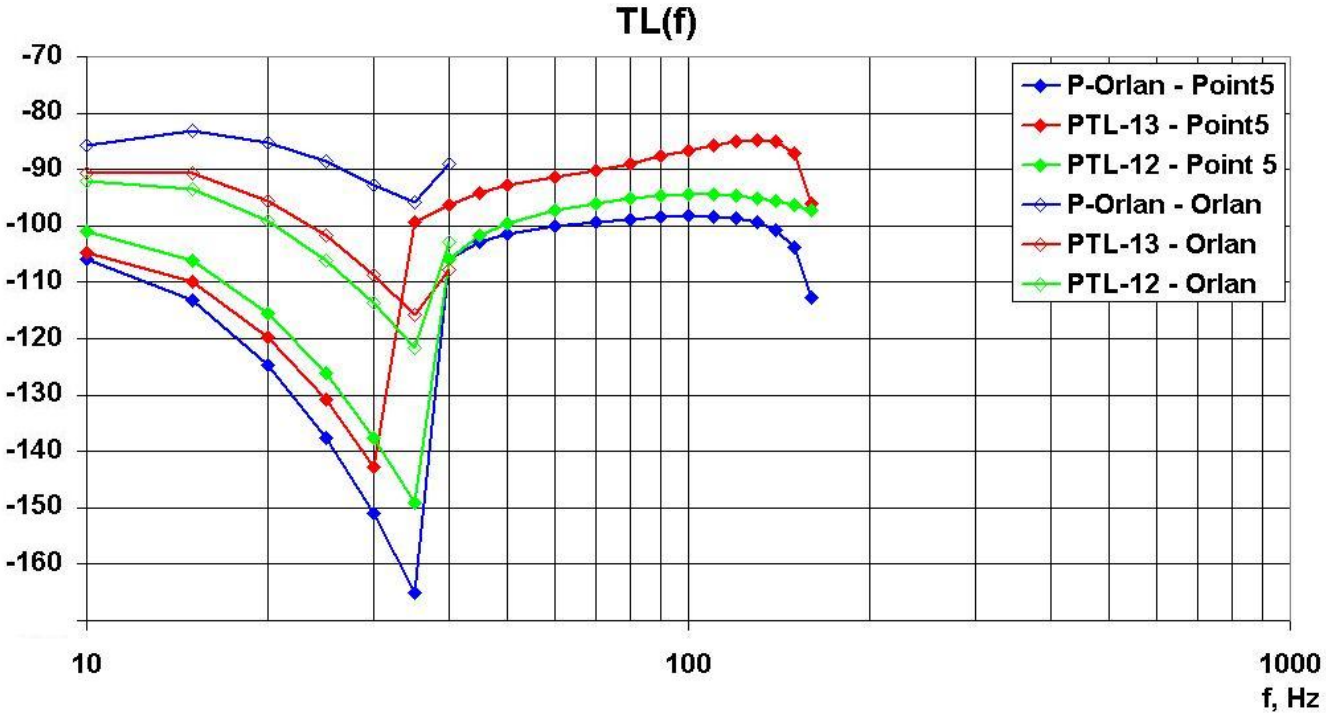

Figure 3.19 - Theoretical TL results estimated along the numerical model waveguides presented in Figure 3.18.

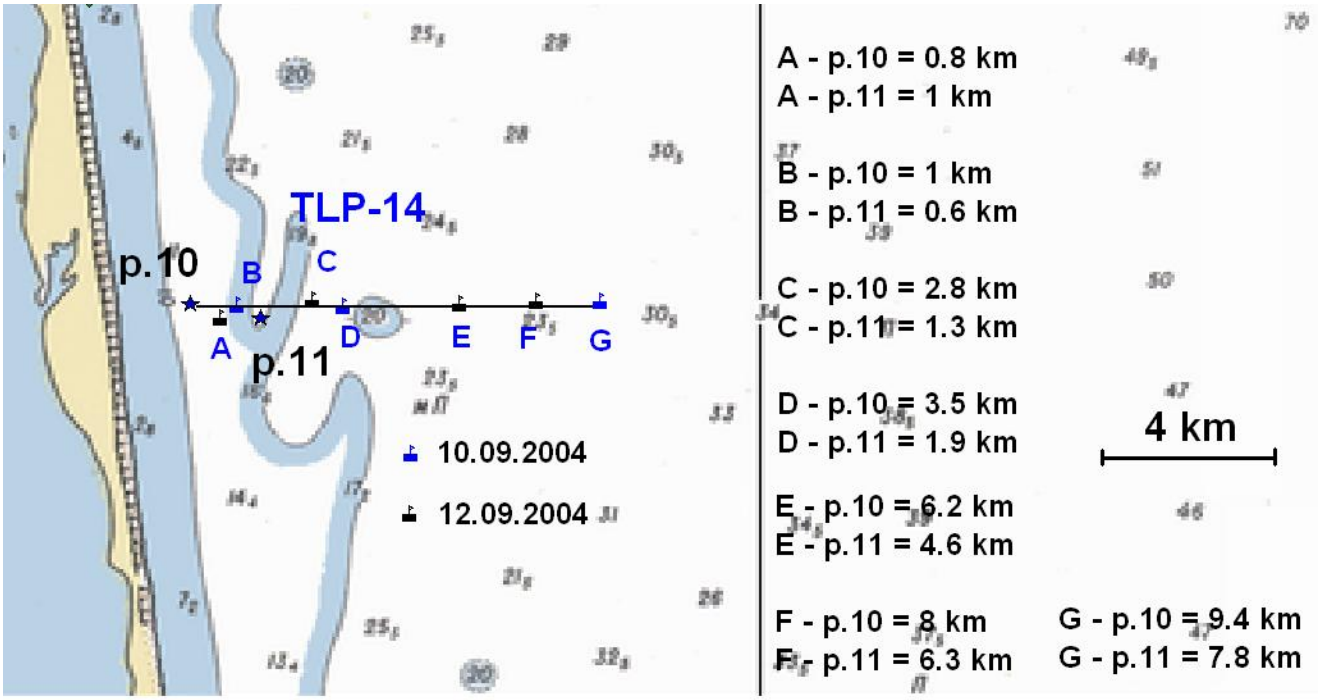

(a.)

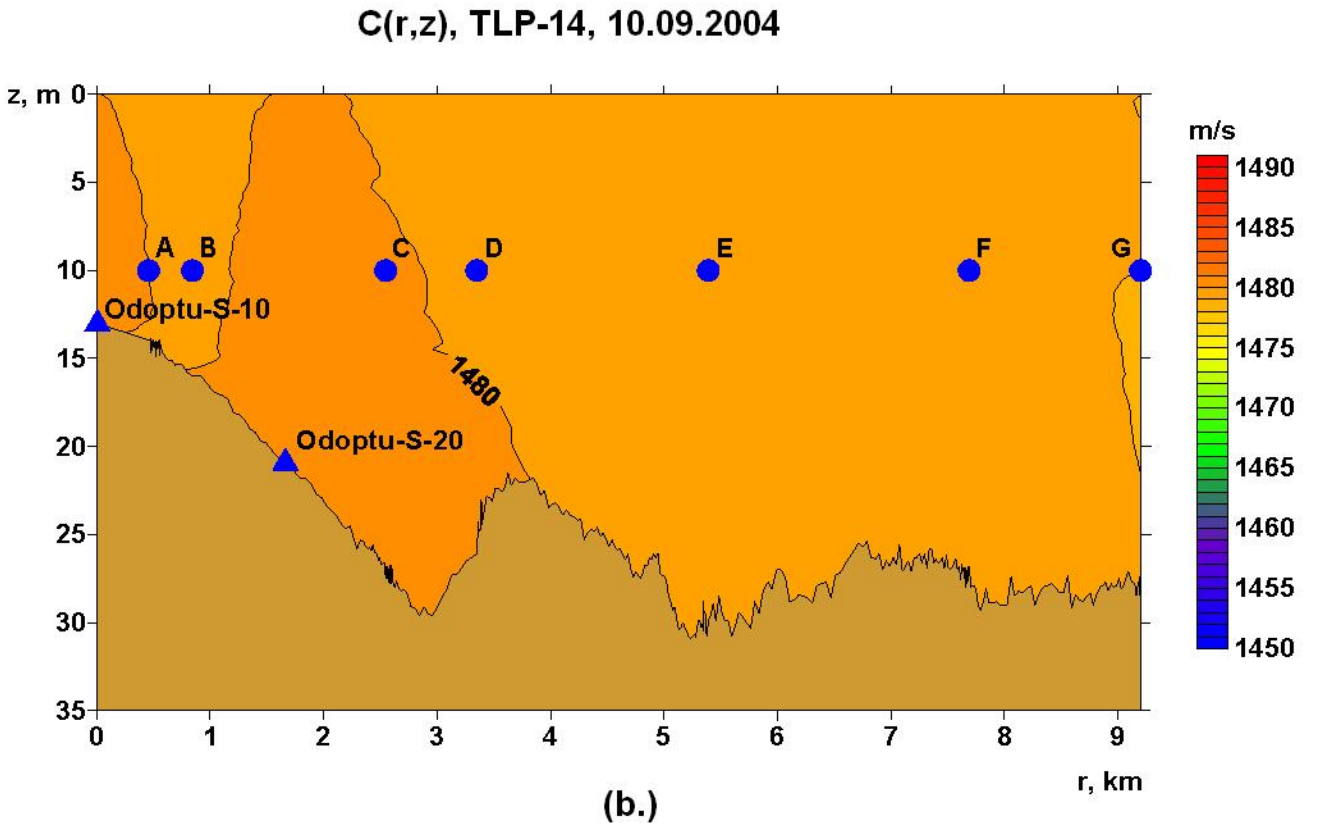

(b.)

Figure 3.20 - TL profile TLP-14 (a) Schematic map showing the experimental layout (b) bathymetry and velocity C(z,r) along the profile as well as the source, receiver and intermediate hydrology locations.

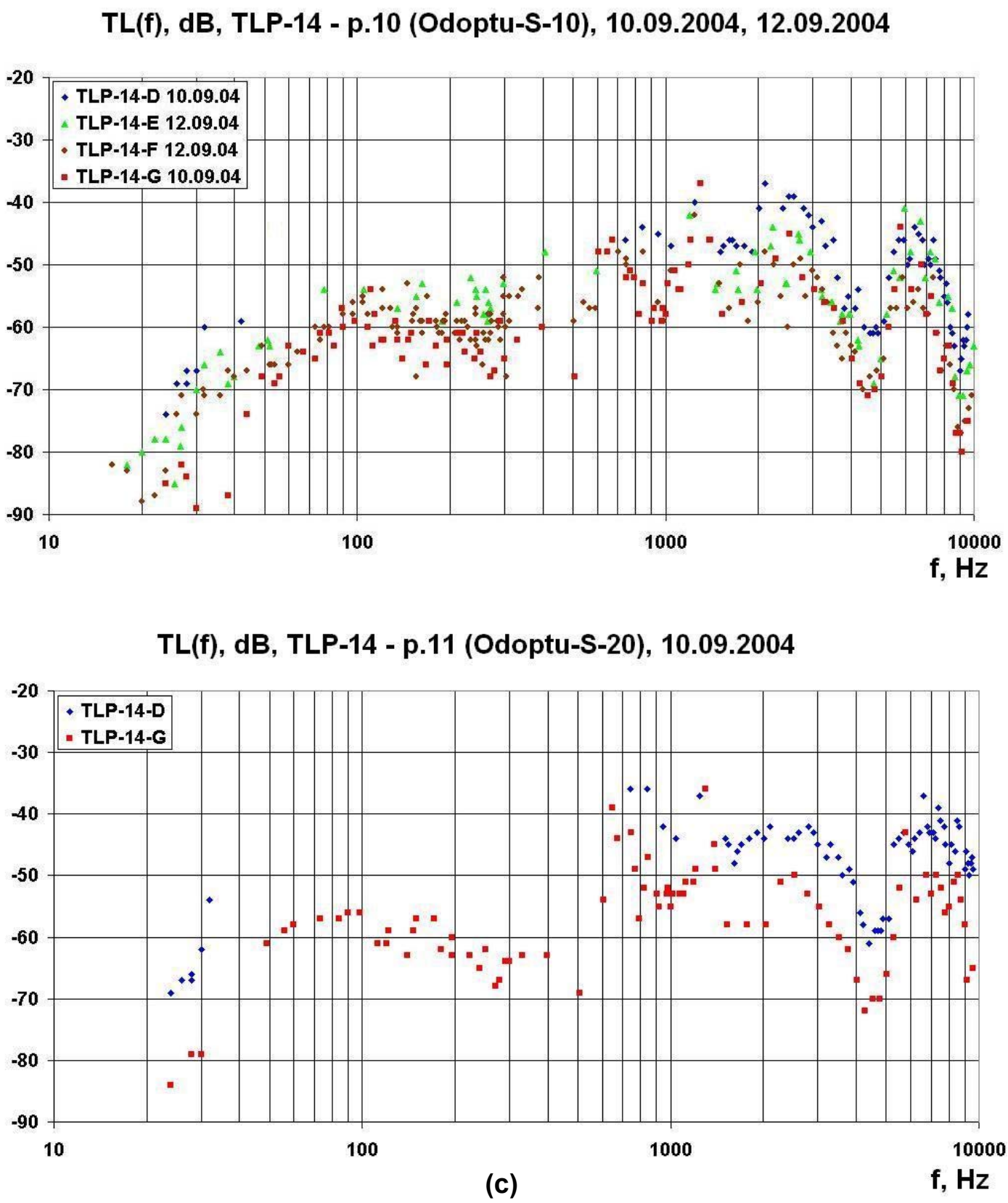

Figure 3.20 - TL profile TLP-14 (c) Frequency dependent TL plot showing the results for both receiver locations (Odoptu-S-10 and Odoptu-S-20).

4 Analysis of acoustic pulses from marine life, anthropogenic and natural seismicity

This section describes the temporal and spectral characteristics of impulses recorded on the NE Sakhalin shelf at different locations and times during the 2004 field season. Similar impulses were reported during the 2003 field season [Borisov et.al., 2004]. These impulses had biogenic, anthropogenic and natural seismicity origins.

4.1 Anthropogenic Impulses

Figure 4.1 is a sonogram *G(f,t)* showing anthropogenic noise from a seismic survey being acquired north of the Odoptu license area and recorded at the Odoptu-S-10 monitor station. The seismic vessel stopped acquiring data at 12:40 on 30 September. Figure 4.2 shows time domain plots *A(t)* of acoustic impulses recorded at the PA-B-20 monitor station. The research vessel *Akademik Shokalskiy* probably generated the anthropogenic impulses seen in Figure 4.2(a) while it conducted engineering surveys along the alternate pipeline routes. Superimposed on the cyclic anthropogenic impulses (S-imp) (Figure 4.2(b)) is a more powerful impulse (Imp) of unknown origin (Figure 4.2(c)). Figure 4.2 shows that the anthropogenic impulse has a duration of approximately 0.5 s, while the unknown impulse (Imp) has a duration of approximately 100 ms.

More complex anthropogenic impulses were recorded at the Orlan monitor station. Figure 4.3 shows time domain plots *A(t)* depicting the structure of these signals. The first pulse (marked Imp) is shown in greater detail in Figure 4.3(b). Detailed analysis of this figure indicates that the impulse is frequency modulated and has duration of approximately 3.5 seconds[27].

4.2 Impulses of possible biogenic origin recorded in 2004

Figure 4.4(a) shows a group of impulses recorded at the PA-B-20 monitor station. Previous experience indicates that this acoustic signal was possibly generated by the activity of a marine animal. Figure 4.4(b) shows that a powerful pulse burst (Imp-1) is assembled from two impulses (Imp-1.1 and Imp-1.2), each with a duration of ~20 ms. The amplitude of the first impulse at the monitor station exceeded 2.4 Pa[28].

[27] The signals were generated by an unknown source that was moving away from the recording station. The data were initially clipped, but later were recorded without clipping (Figure 4.3(c)).
[28] The record was clipped.

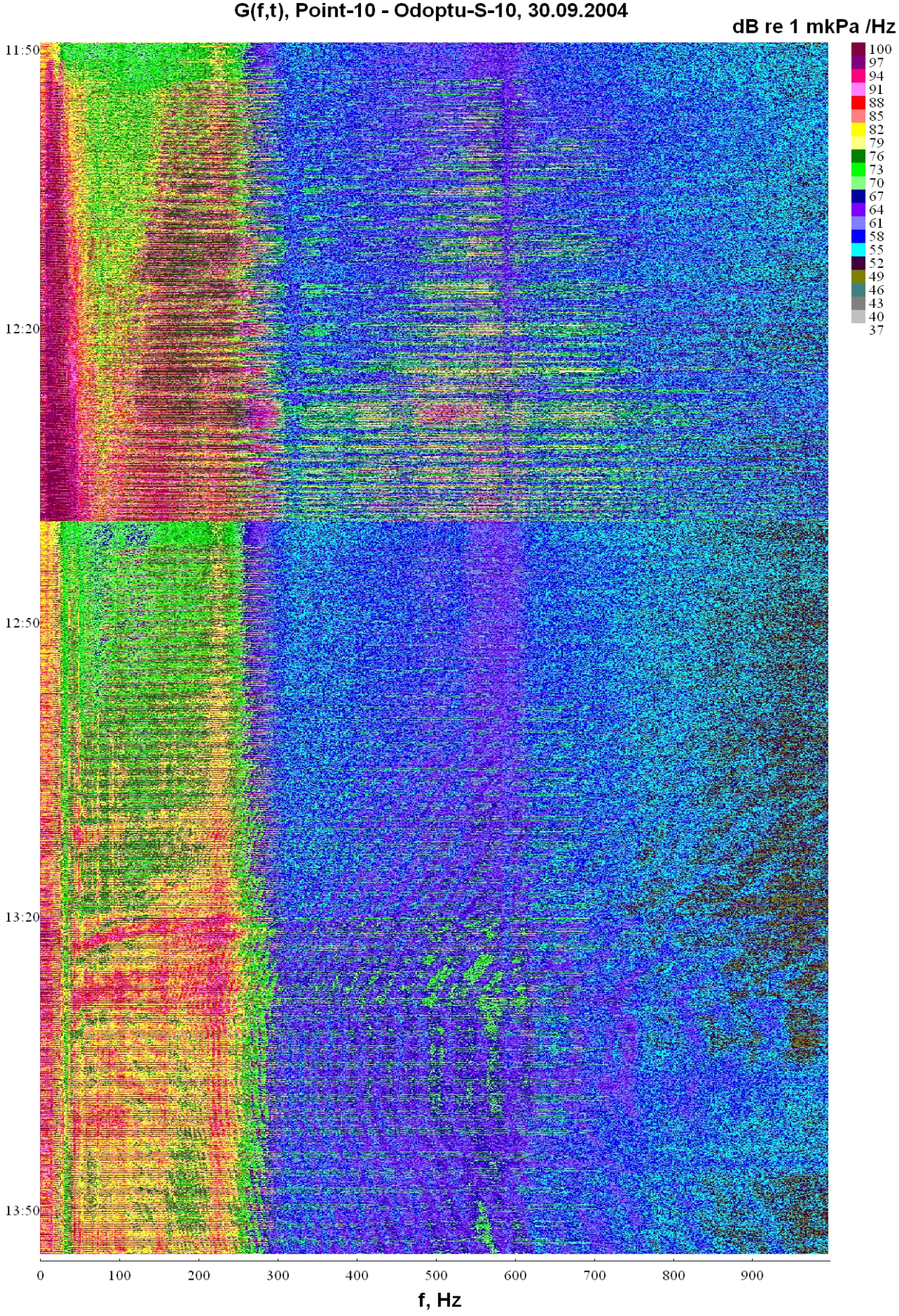

Figure 4.1 - Sonogram *G(f,t)* of data recorded at the Odoptu-S-10 monitor station on 30 September, 2004.

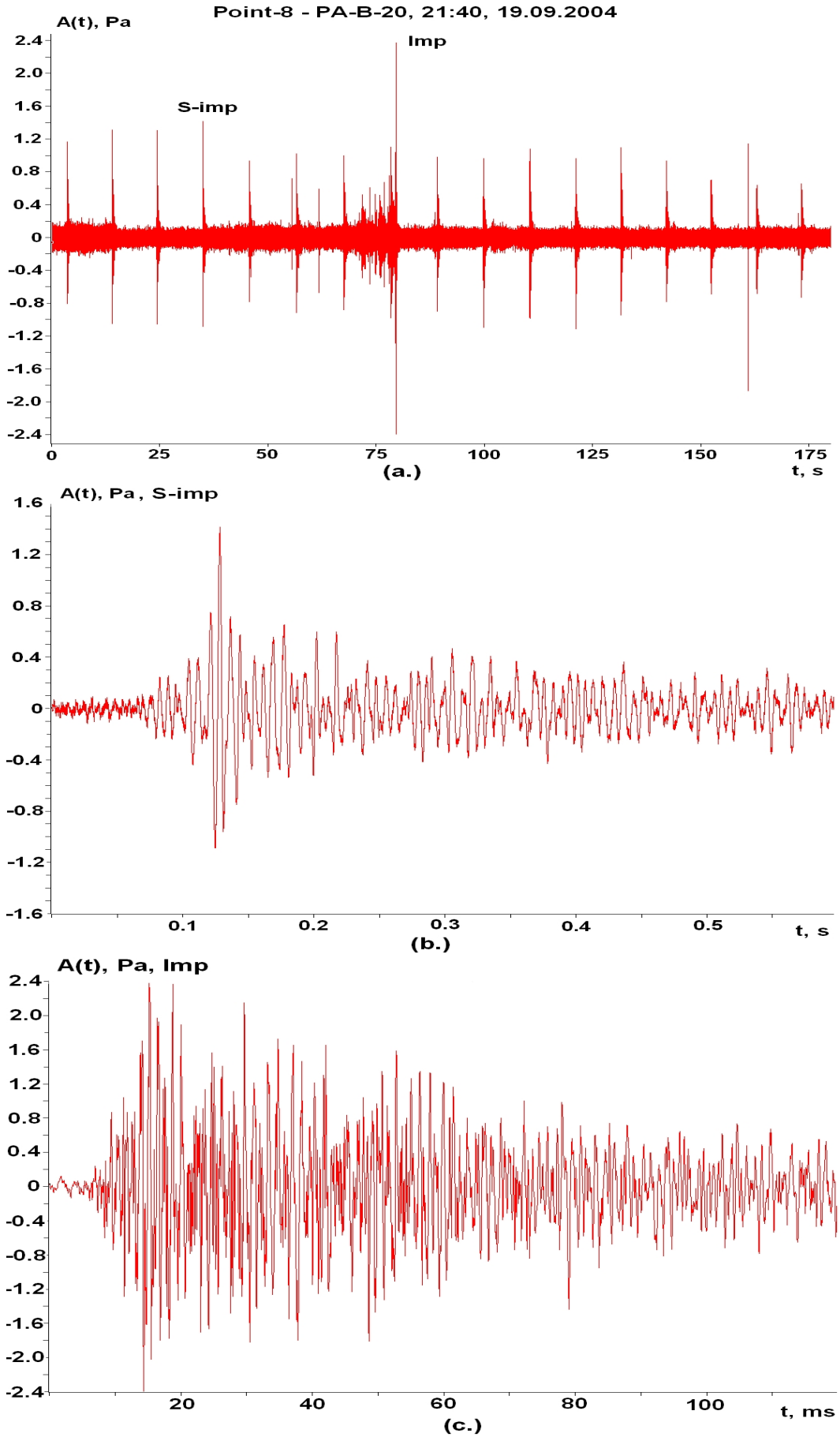

Figure 4.2 - Impulses recorded at the PA-B-20 monitor station on 19 September 2004.

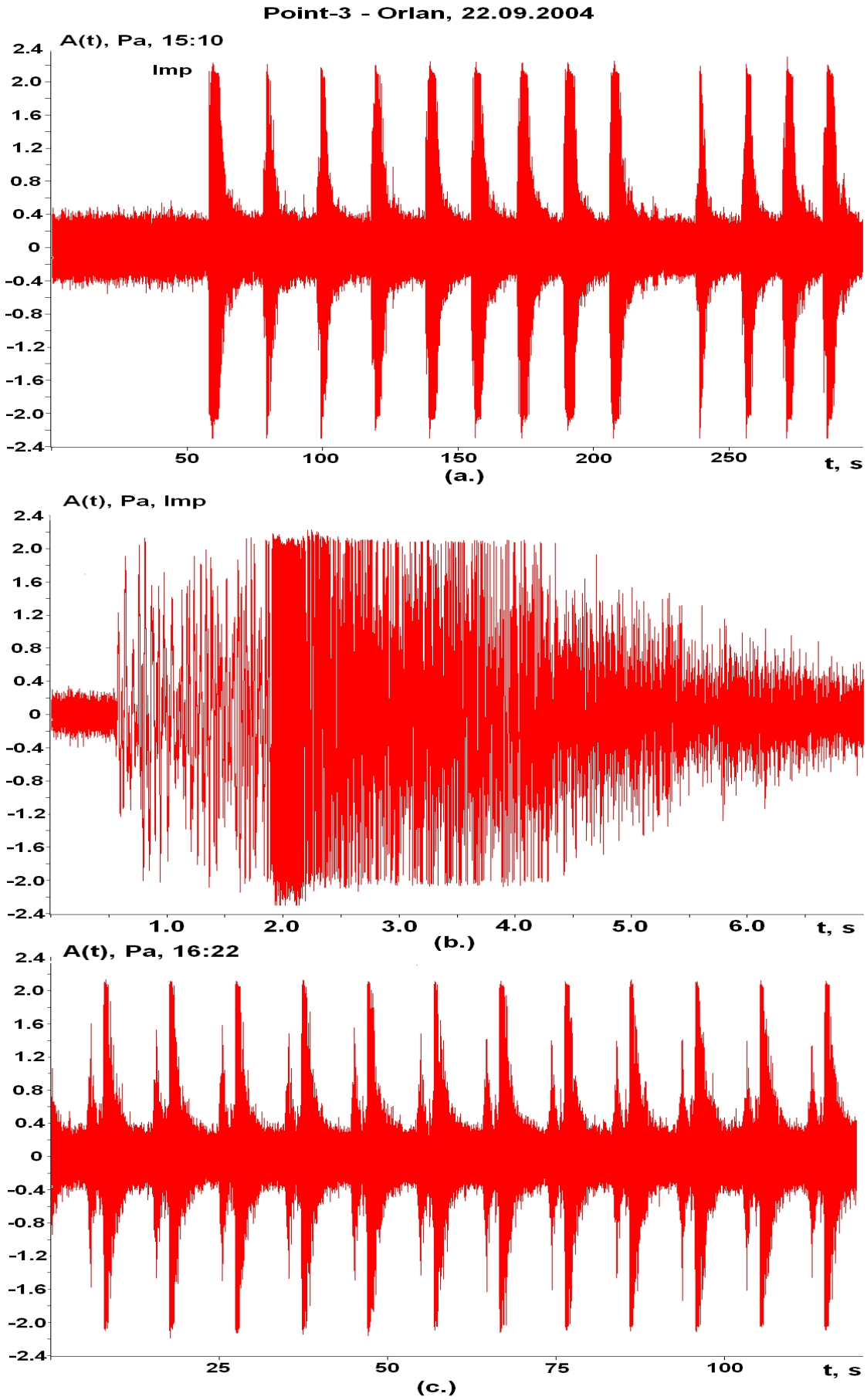

Figure 4.3 - Impulses recorded at the Orlan monitor station on 22 September 2004.

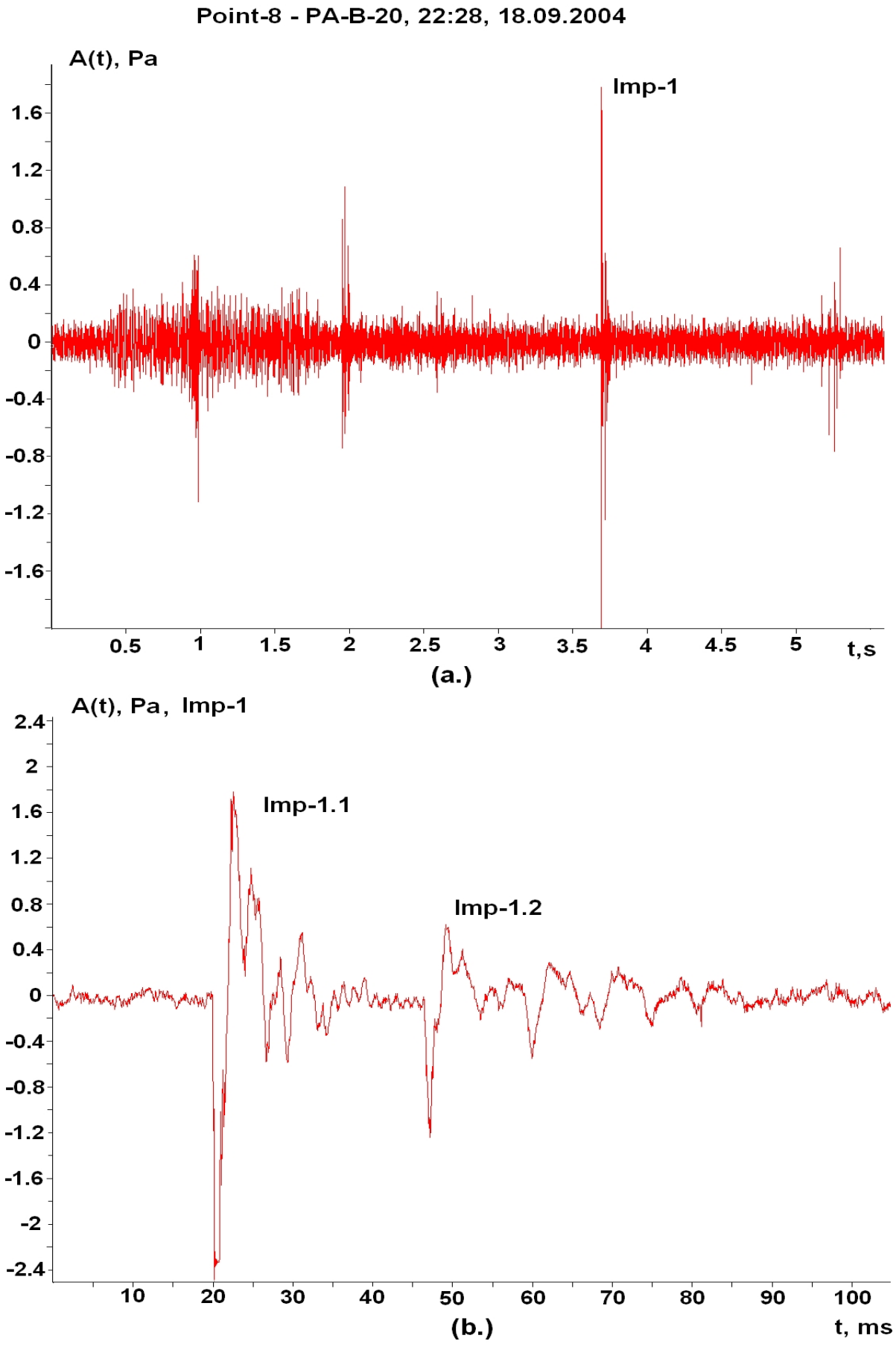

Figure 4.4 - (a) Impulses of biogenic origin recorded at the PA-B-20 monitor station on 18 September 2004 (b) blow up of impulse Imp-1.

Figure 4.5 shows further acoustic impulses, which were possibly generated by marine animals. The time domain amplitude structure of impulse Imp-1 (Figure 4.5(b)) is similar to impulse Imp-1.1 measured at the PA-B-20 monitor station (Figure 4.4(b)), but its duration is almost 10 times shorter. Impulse Imp-2 (Figure 4.5(c)) has a more complex amplitude structure and a duration of ~25 ms.

The acoustic signals plotted in Figure 4.6 were recorded at the Arkutun-Dagi monitor station and are characterized by simple (Figure 4.6(b)), repetitive (Figure 4.6(c)), impulses of relatively large amplitude (more than 2.4 Pa). The impulse duration is approximately 2 ms and the frequency ~500 Hz.

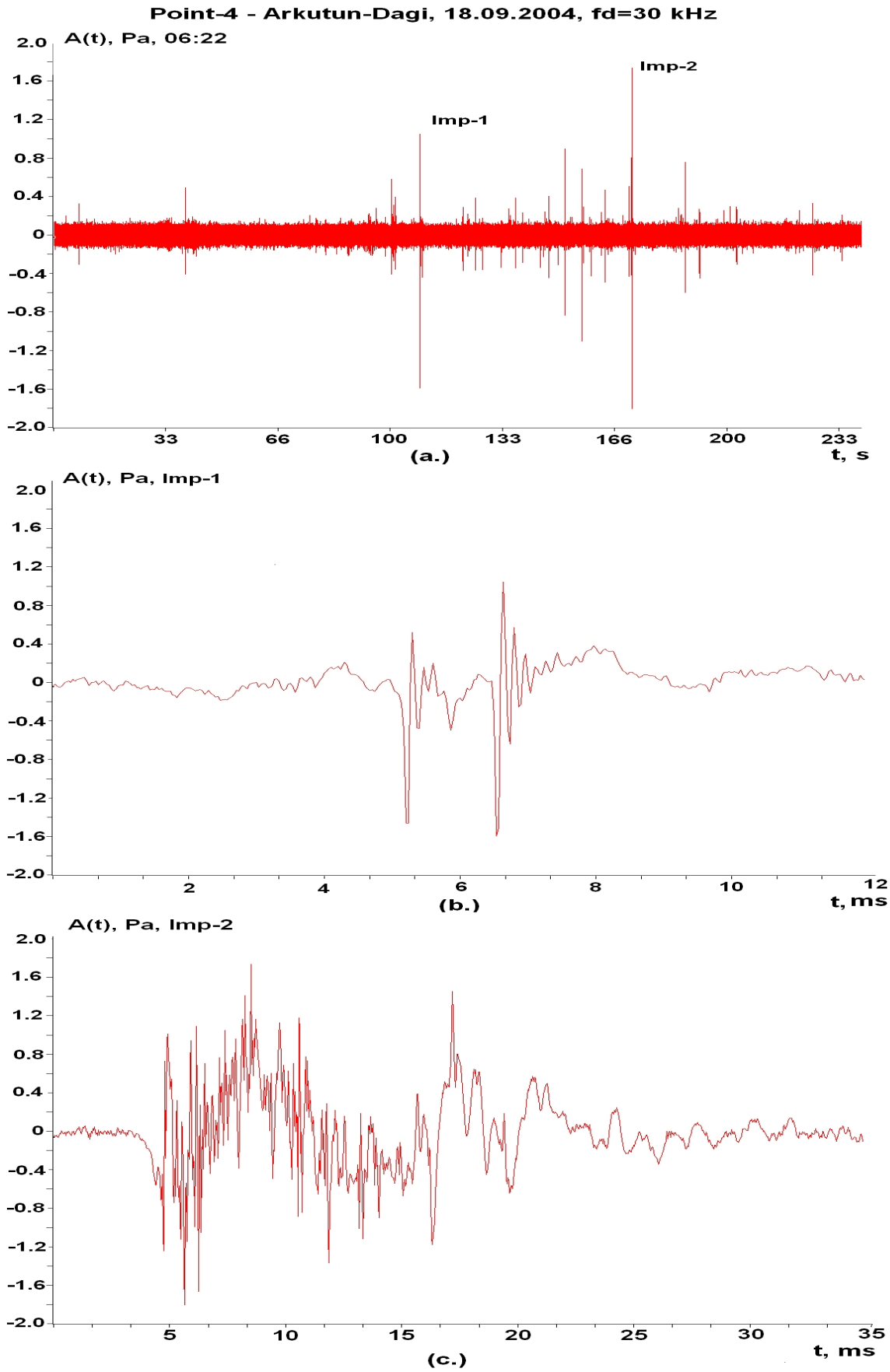

Figure 4.5 - Impulses of biogenic origin recorded at the Arkutun-Dagi monitor station on 18 September 2004.

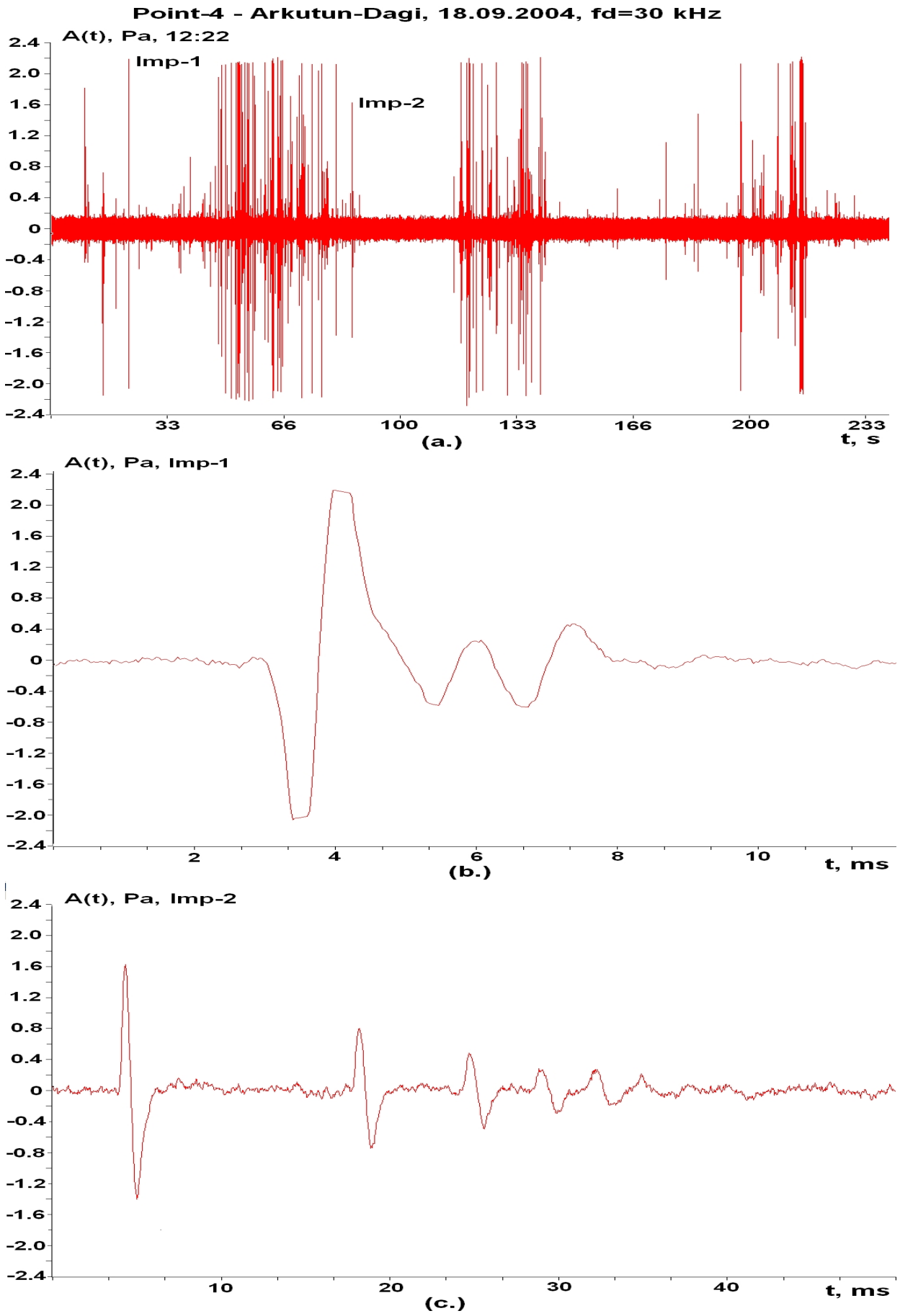

Figure 4.6 - Acoustic pulses of unknown origin recorded at Arkutun-Dagi monitor station on 18 September 2004.